Improving ^{210}Po low level measurements in seawater

López-Rodríguez, Á.[1], González-González, B.[1], García-Prieto, C[1]., Mas, J.L.[2], Le Moigne, F.A.C.[3], Giering S.L.C.[4], Hurtado-Bermúdez, S.[1], Mantero, J.[1], Villa-Alfageme, M.[1*]

1. Dpto. Física Aplicada II, ETSIE, Universidad de Sevilla, 41012 Sevilla, Spain

2. Dpto. Física Aplicada I, ETSII, Universidad de Sevilla, 41012 Sevilla, Spain

3. Laboratoire LEMAR. Institut Universitaire Europén de la Mer. 29280 Plouzané, France

4. National Oceanography Centre, European Way, Southampton, SO14 3ZH. UK

Peer review status:

This is a non-peer-reviewed preprint submitted to Talanta

Abstract

Ocean is the largest sink of atmospheric carbon, atmospheric CO_2 is synthesized by surface phytoplankton into particle organic carbon (POC) that is exported from the ocean surface to depth, where it can be stored for years. An accurate quantification of downward POC flux is crucial for making reliable predictions of present and future atmospheric CO_2 concentrations. A method based on the measurement of the disequilibrium of the radioactive pair ^{210}Pb - ^{210}Po in the seawater column is commonly used to estimate the POC export flux; as ^{210}Po is preferentially scavenged by sinking particles in relation to its parent ^{210}Pb, due to their different biogeochemical behaviour. To quantitatively measure the preferential ^{210}Po scavenging it is necessary to isolate polonium from the aqueous matrix. This is a challenging step in seawater matrices due to its high content in salt content and organic matter, to which ^{210}Po is strongly bound.

We propose an accurate, robust, and easy-to-perform onboard during cruises method for measuring ^{210}Po and ^{210}Pb in seawater using $FeSO_4$ (Fe^{2+}) to coprecipitate polonium as $Fe(OH)_2$, with ^{209}Po as a radioactive tracer. The method was first tested on groundwater and coastal seawater samples from southern Spain and validated with open-ocean samples from two campaigns around the PAP-Site Observatory (48.83° N, 16.5° W) in the North Atlantic. Replicate samples were also processed employing a traditional method based on the co-precipitation using $Fe(OH)_3$ (Fe^{3+}). The results show that the novel method coprecipitation method using $FeSO_4$ (Fe^{2+}) yields activities of ^{210}Po and ^{210}Pb that are consistent with previously reported values. Applying this method, identical activity concentrations of ^{210}Po and ^{210}Pb were observed in deep ocean waters. In these waters no preferential scavenging of ^{210}Po relative to ^{210}Pb should occur, so the secular equilibrium is expected. Contrastingly, when coprecipitation is used with $Fe(OH)_3$ (Fe^{3+}), the activity of ^{210}Po is underestimated by an average of 40 ± 5% in both coastal and open ocean samples, compared to coprecipitation with Fe^{2+}. Furthermore, unexpected ^{210}Po deficits relative to ^{210}Pb were measured in deep ocean waters and secular equilibrium was not detected, evidencing that ^{210}Po is underestimated using this technique.

Keywords

Polonium, radioactive disequilibrium, ^{210}Po - ^{210}Pb, ocean carbon storage, biological pump, radiochemical speciation, α-spectrometry

1. Introduction

The ocean is the largest active sink for carbon dioxide, and the Biological Carbon Pump (BCP) is one of the main mechanisms by which CO_2 is removed from the atmosphere and exported to the deep ocean as particulate organic carbon (POC) over seasonal to decadal timescales. This POC is transported in the form of sinking particles that constitute marine snow (Sanders et al., 2014). Approximately 5-20 GTC yr^{-1} are exported from the surface to deep ocean by means of the BCP (Henson et al., 2022; Puigcorbé et al., 2020). Suppressing this mechanism could increase atmospheric CO_2 levels up to 50% (Le Moigne, 2019; Sanders et al., 2014). Therefore, to make reliable predictions regarding the evolution of atmospheric CO_2, it is necessary to accurately quantify how much POC is exported and storage by oceans through the BCP. One of the main vectors of the BCP to sequester the POC is the gravitational pump, that accounts for the downward POC fluxes due to particles sinking by gravity (Boyd et al., 2019)

A widely used approach to estimate downward POC fluxes is based on the different biogeochemical behaviour of ^{210}Po and ^{210}Pb in the water column. In the euphotic zone (EZ), the layer where phytoplankton synthesizes atmospheric carbon (Villa-Alfageme et al., 2024), a ^{210}Pb – ^{210}Po disequilibrium arises from the preferential scavenging of ^{210}Po, relative to ^{210}Pb, by sinking organic matter (Le Moigne et al., 2013). In the upper Twilight Zone (TZ, < 200 m), ^{210}Po excesses are attributed to remineralization and fragmentation processes carried out by bacteria and zooplankton (Villa-Alfageme et al., 2014). Deeper in the TZ, the two ^{210}Po and ^{210}Pb are expected to reach secular equilibrium (i.e., equal activities), because no additional export and remineralization processes, and so additional ^{210}Po inputs or losses, take place (Ceballos-Romero et al., 2016).

^{210}Po is commonly determined by alpha spectrometry due to its low detection limits (Villa-Alfageme et al., 2016). Before the radiochemical preparation ^{210}Po must be extracted, isolated and concentrated from the sampled matrix. In seawater, ^{210}Po extraction is particularly challenging because of the complexity of this matrix, which contains high salt concentration and organic matter to which ^{210}Po is strongly bound (Stewart et al., 2007; Villa-Alfageme et al., 2016).

During oceanographic cruises this extraction method must be performed on board to minimize the time elapsed between sample collection and ^{210}Po determination. This preserves the ^{210}Pb – ^{210}Po disequilibrium in the water column, because of the relatively short ^{210}Po half-life ($T_{1/2}$=138 days). Furthermore, as storing 5L of water per depth on board is logistically challenging, the extraction step should also concentrate the sample, reducing the initial 5 L samples to 250 mL. Therefore, the methods for measuring ^{210}Po in oceanography must be robust, straightforward and quick to implement on board, in order to save time working at sea.

A traditional method for ^{210}Po extraction is based on its coprecipitation, together with a tracer isotope, normally ^{209}Po (Roca-Martí & Puigcorbé, 2024; Thakur & Ward, 2020), with a precipitating agent (e.g. Roca-Martí & Puigcorbé, 2024), typically $Fe(OH)_3$, i.e. using Fe^{3+} (e.g. Matthews et al., 2007). A second well established method is the cobalt–ammonium pyrrolidine dithiocarbamate, Co-APDC, precipitation method, frequently used in the past (Fleer & Bacon, 1984). While this approach is robust and has proven to provide solid results in the determination of ^{210}Po and ^{210}Pb in seawater (e.g. Roca-Martí et al., 2021), it is a laborious and time-consuming method to apply on board during oceanographic cruises.

For the method based on polonium coprecipitation using Fe^{3+}, there is extensive literature reporting analytical problems in the measurement of ^{210}Po and its disequilibrium in depth with ^{210}Pb in seawater matrices. Results from previous intercalibration studies (Chung & Craig, 1983; Church et al., 2012; Cochran et al., 1983, Scripps, Yale, and Woods Hole) and several oceanographic cruises (Ceballos-Romero et al., 2016; Kim., 2001.; Kim et al., 1999; Rigaud et al., 2015; Roca-Martí et al., 2021) pointed out that ^{210}Po and ^{210}Pb do not consistently reached the expected secular equilibrium in deep waters when the Fe^{3+} method is used. For this reason, some authors suggest that this method underestimates ^{210}Po activity in the samples (Roca-Martí et al., 2021) and this prevents reaching equilibrium in depth with its parent ^{210}Pb.

This is an important issue for downward POC flux evaluations, as the analytical inaccuracies in ^{210}Po and ^{210}Pb activity determination are directly propagated to the accuracy of the POC fluxes derived from this method (e.g. Church et al., 2012)

Hence, in recent years, there has been a growing interest in developing new alternative, reliable methodologies to accurately, precisely and routinely measure ^{210}Po in seawater samples (e.g. Katzlberger et al., 2001; Kim et al., 1999; Vajda et al., 1997; Waples, 2020; Waples et al., 2025). In this study, we propose a novel, robust, and easy to apply on-board method for the accurate determination of ^{210}Po and ^{210}Pb activities in seawater, based on the coprecipitation of ^{210}Po and ^{209}Po with $FeSO_4$ (Fe^{2+}). This method has been successfully applied for the determination of other actinides, such as ^{236}U and ^{237}Np, in seawater (Chamizo et al., 2016; López-Lora et al., 2019, 2020).

To establish this novel method, ^{210}Po was determined on different water matrices, including groundwater and coastal surface seawater samples collected from southern Spain. To broaden the method, it was applied to open-ocean seawater samples collected during two oceanographic campaigns around the PAP-Site Observatory (48.83º N, 16.5º W), in the North Atlantic, to obtain high-resolution ^{210}Po – ^{210}Pb depth profiles. For comparing and validating the performance of the results, several replicates were collected and processed using the traditional Fe^{3+} method.

2. Sampling and methods

2.1. Sampling

To set up and validate the novel method, a total of 94 samples from different unfiltered water matrices — including freshwater from wells, coastal surface and open-ocean samples — were collected and ^{210}Po, and sometimes ^{210}Pb, were measured using our novel method using $FeSO_4$ (Fe^{2+}) coprecipitation.

Furthermore, to demonstrate the robustness of this Fe^{2+} method, different elapsed times between sampling, processing, and measurement were tested. These included immediate ^{210}Po determination, one-year storage, and a dual approach to determine both ^{210}Po and ^{210}Pb. The equations used to determine ^{210}Po and ^{210}Pb with these approaches are described in Section 2.3.

A comprehensive and exhaustive analysis, encompassing a wide range of water matrices and different elapsed times in ^{210}Po determination, was carried out to validate this method, despite the lack of available, accurately evaluated, reference water matrices for ^{210}Po.

Samples were acidified to pH 3 immediately after collection for preservation and avoiding wall adsorption using ~ 10 ml HNO_3 for a 5 L sample. Samples were also spiked with 0.2 Bq ^{209}Po for 5 L to assess polonium recovery after the radiochemical procedure. A minimum of six hours was allowed for homogenization to take place.

To test the performance and robustness of Fe^{2+} method, we determined ^{210}Po activity in different water matrices– groundwater, coastal surface seawater and open-ocean seawater – allowing three different elapsed times between collection and measurement (immediate measurement and long elapsed time and intermediate elapsed time measurements).

2.1.1. Freshwater

Three locations were sampled for 1 L groundwater collection near a closed uranium mine in Jaén, Spain, currently under decommissioning. Samples were collected during the PVRA environmental radiological monitoring program of the Consejo de Seguridad Nuclear (CSN) in January 2021. Sampling coordinates are shown in Figure S1 (Supp. Material). Groundwater samples were stored for one year after collection before ^{210}Po determination.

The unfiltered water volumes collected in the three sampling points were split into 1 L aliquots and grouped into batches denoted as A, B, and C (Table 1). Half of the aliquots from each batch were processed using the Fe^{2+} method, and the other half were replicates processed using the Fe^{3+} method for intercalibration.

2.1.2. Coastal surface seawater

5 L Coastal surface seawater samples were collected in the Gulf of Cádiz, Spain, in Huelva, in December 2021, and in Cádiz in March 2022. Sampling coordinates are shown in Figure S1.

These unfiltered samples were split into 5 L aliquots and grouped in different batches. The total sample volume collected in Huelva was split into 4 aliquots (Batch D, Table 1), and the sample volume from Cádiz into 18 aliquots, grouped into Batches E to H. Half of

the aliquots from each batch were processed using the Fe^{2+} method, while the replicates were processed using the Fe^{3+} method for intercalibration. In these samples, a single measurement for ^{210}Po determination was performed immediately after collection.

2.1.3. Open-ocean seawater profiles

To test the Fe^{2+} method open ocean seawater, a total of 87 samples from 0 to 600 m depth with a CTD-rosette and Niskin bottles were collected in two different oceanographic cruises at the Porcupine Abyssal Plain Observatory (PAP-Site, 48º 50′ N 16º 30′ W, 4850 m depth) to obtain high resolution ^{210}Po - ^{210}Pb depth profiles. This observatory is a multidisciplinary open ocean long-term series site in the NE Atlantic focused on the study of the connections between the surface and the deep ocean (e.g. Hartman et al., 2021).

An unfiltered water profile was collected during the *JC231* cruise, on 18 May 2022, on board the *RRS James Cook* led by the National Oceanography Centre (NOC). The goal of the cruise was to continue time-series observations on the surface ocean, water column, and seafloor at the site. The station sampled during this campaign was labelled SS1-1 (Table S1, Figure 1).

Five additional profiles were sampled the following year, between 6 June and 17 July 2023, on board *Pour Quoi Pas?* during APERO cruises. APERO project aims to study the mechanistic functioning of the BCP with emphasis on the mesopelagic ocean. Stations sampled during this campaign were labelled from SS1 to SS5 (Table S1, Figure 1).

Replicates were collected at several depths in both cruises and processed using the Fe^{3+} coprecipitation method (Table S1). A double-measurement approach was applied to these samples to determine both ^{210}Po and ^{210}Pb activities (See section 2.3.4.).

2.2. $Fe(OH)_2$ coprecipitation method

Below we describe the steps followed for ^{210}Po determination in 5 L water samples

Step 1. *Preconcentration of lead and polonium*

· Add the carrier, 1.25 g $FeSO_4$ (Fe^{2+}), and 2.5 g $K_2S_2O_5$ to prevent Fe^{2+} from oxidizing

· Shake vigorously

· Adjust pH to 8-9 with NH_4OH → Coprecipitation of polonium and ^{210}Pb with $Fe(OH)_2$

· Let the precipitate settle for at least 24 hours

· Siphon and extract the supernatant to 250 ml.

Step 2. *Sample conditioning*

·Evaporate the precipitate to near dryness

·Dissolve the precipitate using 10 ml 37% HCl and 1 ml H_2O_2

·Repeat the evaporate-dissolve process three times to digest the organic matter and convert to chloride medium

·Dissolve the final residue in 120 ml 1M HCl

Step 3. *Separation of polonium from lead*

·Add ascorbic acid to secure that iron is reduced to Fe^{2+}

·Self-deposit ^{209}Po and ^{210}Po onto one-side coated silver disc (25 mm diameter) at 60 – 70ºC with constant stirring for at least 8 hours

An intercalibration between methods was performed using Fe^{3+}. In this case, Steps 2 and 3 remained the same, while Step 1 employed $FeCl_3$ (Fe^{3+}) as carrier. Specifically, 10 mL (0.250 g/mL) of $FeCl_3$ were added. $Fe(OH)_3$ and polonium were coprecipitated after adjusting the pH to 8–9 with 20 mL of NH_4OH (e.g. Villa-Alfageme et al., 2016).

2.3. Instrumentation and α – measurement

^{209}Po and ^{210}Po activities were determined at CITIUS (Centro de Investigación, Tecnología e innovación, Universidad de Sevilla) laboratory at the Universidad de Sevilla by alpha spectrometry using PIPS detectors with 450 mm² active area and 18 keV resolution at the highest alpha emission energy of ^{241}Am (5.486 MeV) for at least one week to guarantee that uncertainties were lower than 5%. The alpha background count rates (cps) contributed on average less than 1% to the total counts of ^{210}Po and ^{209}Po (10^{-6} cps for ^{210}Po and 10^{-5} cps for ^{209}Po).

Decay corrections are applied according to the different time intervals between sample collection and measurement. Equations for ^{210}Po determination and the associated decay corrections are presented in the next section.

2.4. ^{210}Po and ^{210}Pb determination

2.4.1. α-spectrometry and chemical yield

^{210}Po activity in the water samples analysed in this study was measured by alpha spectrometry, a widely used technique for low-level ^{210}Po determination in water (Villa-Alfageme et al., 2016).

To determine ^{210}Po activity by α-spectrometry, it is necessary to first isolate it from the aqueous matrix using a radiochemical method. Radiochemical isolation leads to partial loss of the isotope initially present. To account for these losses an isotope with similar, ideally identical, chemical behaviour must be added. For ^{210}Po, the most widespread spike is ^{209}Po (Roca-Martí & Puigcorbé, 2024). Using this internal tracer ^{210}Po activity concentration (A_{210Po}) is determined following,

$$A_{210Po} = \frac{N_{210_{Po}} \cdot V_{209_{Po}}}{N_{209_{Po}} \cdot V_S} \cdot A_{209_{Po}} \quad (1)$$

Where $n_{210_{Po}}$ refers to ^{210}Po counts in the detector spectra (cps) background corrected and V_s to sampled volume.$n_{209_{Po}}$ refers to ^{209}Po count rate in the detector spectra (cps), background corrected, $A_{209_{Po}}$ is the activity of the spike initially added and $V_{209_{Po}}$ is the volume of spike added.

The fraction of radioisotope recovered at the end of the method is known as chemical yield (R). It can be estimated from $A_{209_{Po}}$ following,

$$R = \frac{N_{209_{Po}}}{\epsilon_\alpha \cdot A_{209_{Po}} \cdot V_{209_{Po}}} \quad (2)$$

Where ε_α is α counting efficiency.

2.4.2. ^{210}Po determination in immediate measurements

Coastal surface seawater samples from Huelva and Cádiz were treated and measured immediately after collection for ^{210}Po determination.

Both ^{210}Po and ^{210}Pb are in all water matrices, and if the measurement is performed few days after collection, the measured ^{210}Po correctly corresponds to its activity at the sampling date, since the amount of ^{210}Po derived from the ^{210}Pb decay is negligible during the immediate measurements. In that case equation (1) can be used directly, corrected by the elapsed time between the ^{210}Po isolation date into the silver disk and the measurement date.

2.4.3. ^{210}Po determination after a long time period (secular equilibrium with ^{210}Pb)

Groundwater samples collected in Jaén (Spain), were stored for one year after collection, it was then that ^{210}Po determination was performed from a single measurement.

When the elapsed time between collection and measurement exceeds several half-lives of ^{210}Po ($T_{1/2} = 138$ days), ^{210}Po and ^{210}Pb reach secular equilibrium (i.e., the same activity for parent and daughter). Therefore, when groundwater samples were measured ^{210}Po and ^{210}Pb were in near-secular equilibrium, meaning that the ^{210}Po and ^{210}Pb activities in the sample coincided and were constant in the measurement time frame (provided that $T_{1/2} = 22.3$ years). Equation (1) calculates activity for ^{210}Po that is equal to that of ^{210}Pb, the activity is corrected by the elapsed time between the ^{210}Po isolation date into the silver disk and the measurement date.

2.4.4. ^{210}Po and ^{210}Pb determination after an intermediate time period (not secular equilibrium with ^{210}Pb)

PAP cruises lasted approximately 15 and 40 days, respectively. The open ocean samples collected at NOC and APERO campaigns were measured one-three months after

collection and ^{210}Po and ^{210}Pb coprecipitation. That means that after that time period in the sample there was a non-negligible amount of ^{210}Po originated by ^{210}Pb decay that must be subtracted from the ^{210}Po measurement to obtain the real ^{210}Po concentration. In those cases, it is possible to apply a double-measurement approach to obtain both ^{210}Po and ^{210}Pb activities at the sampling date Rigaud et al., (2013).

Therefore, ^{210}Po activity at the sampling date ($A_{210Po}(t_s)$) corresponds to the ^{210}Po activity obtained in the first measurement (t_1) subtracting the ^{210}Po contribution from ^{210}Pb decay during the elapsed time between collection and measurement (A_{PoPb}), decay-corrected to the sampling date, equation (S1).

To determine $A_{PoPb}(t_1)$, a cleaning autodeposition is performed after the first measurement to remove any residual ^{210}Po and ^{209}Po not deposited on the disc in the first autodeposition. Uncoated discs are used in this step to maximize Po recovery. The sample is then stored for at least six months, allowing ^{210}Pb to decay into ^{210}Po and ensuring good counting statistics. During this period, all ^{210}Po present in the sample is derived from ^{210}Pb decay. A third deposition onto a coated silver disc is then made.

A second measurement (t_2) is then performed to determine $A_{PoPb}(t_1)$ from $A_{210Po}(t_2)$ using a third-order Bateman equation, equation (S2). ^{210}Pb at the sampling date, ^{210}Pb (t_s), is determined using a similar Bateman equation decay corrected, equation (S3). Finally, ^{210}Po at the sampling date is obtained from equation (S1).

3. Results

3.1. ^{210}Po in groundwater and coastal surface seawater samples

Table 1 presents ^{210}Po activity concentrations and the average of each batch for groundwater and coastal surface seawater samples following our Fe^{2+} coprecipitation method described in Section 2. This table includes also the results from replicates processed using Fe^{3+}.

Groundwater aliquots are representative of their respective batches with the Fe^{2+} method, since batches average standard deviation align with the individual aliquot uncertainties. The only exception was observed in Batch C, with one duplicate showing a markedly higher activity, 18 ± 2 Bq·m^{-3}, whereas the other replicates in the same batch yielded values much closer to those of the remaining batches.

For coastal surface seawater average ^{210}Po standard deviation also aligns with individual aliquots uncertainties in all batches. Batches of seawater samples from Cádiz were measured in consecutive weeks. A small, but not negligible, fraction of the determined ^{210}Po therefore originated from ^{210}Pb ingrowth in the elapsed time between collection and measurement. This is the reason for the slightly increasing ^{210}Po activity obtained with both methods from batches E to G, although they were obtained from the same sample matrix and the sampling time was identical. Note that, in contrast, replicates in the same

batch were measured on the same day and the results are comparable within the same batch.

Regarding the precision of the measurements in the replicates processed using the Fe^{3+} method, the results were generally consistent with those obtained using the Fe^{2+} method. Specifically, the average standard deviation of each batch agreed with the individual uncertainties of the aliquots, with the only exception of Batch C, where precisely the high ^{210}Po activity measured in one replicate (22 ± 4 Bq·m^{-3}) was consistent with the similarly high activity obtained in the corresponding replicate processed with the Fe^{2+} method (18 ± 2 Bq·m^{-3}).

3.2. ^{210}Po – ^{210}Pb depth profiles from PAP-Site campaigns

Figure 2 plots with straight lines ^{210}Pb – ^{210}Pb depth profiles obtained from both NOC (SS1-1) and APERO (SS1 to SS5) campaigns using Fe^{2+}. Depth profiles obtained from the collected replicates processed with the Fe^{3+} method are also shown with dashed lines. See complete dataset in Table S1.

To correctly interpret these depth profiles, we differentiate two regions in the sampled water column. The euphotic zone (EZ), from 0 to 126.5 m at the sampled stations, is the layer that receives enough solar radiation to allow phytoplankton photosynthesis and therefore the production of organic matter (e.g. Marra et al., 2014). The euphotic zone base (EZB, also shown in Figure 2) is taken as the depth of 0.1% light penetration (e.g. Ceballos-Romero et al., 2016). In the twilight zone (TZ), below the EZB, there is no further production of organic matter (e.g. Buesseler et al., 2020).

Table S1 includes also ^{210}Po/^{210}Pb ratios at depth. ^{210}Po/^{210}Pb ratios in the EZ range from 0.59 – 0.93 (average 0.77 ± 0.12) with the Fe^{2+} method. As further discussed in Section 4.2, ^{210}Po deficits in the EZ reflect the preferential ^{210}Po scavenging in the sinking particulate matter relative to ^{210}Pb (e.g. Le Moigne et al., 2013).

In the TZ, ^{210}Po and ^{210}Pb are near secular equilibrium (i.e., ^{210}Po/^{210}Pb ≈ 1), with average ^{210}Po/^{210}Pb ratios ranging from 0.74 to 1.6 (average 1.1 ± 0.3). This secular equilibrium is consistently maintained throughout the entire TZ in SS1-1 and SS5. ^{210}Po excess values (^{210}Po/^{210}Pb > 1) likely reflect the release of particulate ^{210}Po into non-sinking phases through remineralization or disaggregation processes, mainly driven by bacterial and zooplankton activity (e.g. Villa-Alfageme et al. 2014).

Replicates processed with Fe^{3+} also showed ^{210}Po deficits in the EZ, except in SS3 with ^{210}Po/^{210}Pb ratios averaging 1.3 ± 0.4. In the remaining stations average ^{210}Po/^{210}Pb ratios in the EZ range from 0.35 – 0.75 (average 0.59 ± 0.20). In the TZ, average ^{210}Po/^{210}Pb ratios range from 0.49 – 0.99 (average 0.80 ± 0.20)

3.3. Chemical yields

Table 1 shows individual chemical yields determined in samples replicates, along with chemical yield batch averages in groundwater and coastal surface seawater samples. Table S1 summarizes the station-average chemical yields obtained for the collected open ocean samples from PAP cruises.

Chemical yields were higher with the Fe^{2+} method in groundwater samples, ranging from 51 – 68 % (average 57 ± 6 %) relative to coastal and open-ocean samples, which ranged from 31 – 59 % (average 46 ± 9 %).

In the replicates processed using the Fe^{3+} method, no differences in relation to Fe^{2+} were observed in the range of chemical yield values obtained in the different water matrices analysed, ranging from 36 – 67% (average 53 ± 10 %) for groundwater samples and from 40 – 73% (average 54 ± 8 %) for coastal and open-ocean water samples.

4. Discussion

4.1. Performance of Fe^{2+} method

4.1.1. Groundwater and coastal surface seawater

Groundwater samples were stored one year after collection and ^{210}Po and ^{210}Pb reached near secular equilibrium. Therefore, the determined ^{210}Po activity corresponds to that of ^{210}Pb. These samples were collected in the influence area of the Uranium Factory of Andújar (FUA), in Jaén (Figure S1), which is currently under decommissioning. In areas where uranium is mined and extracted, ^{210}Po and ^{210}Pb tend to accumulate in tailings and run-off (Sharma et al., 2021).

Nevertheless, overall, ^{210}Pb activity concentrations measured in the analysed samples do not indicate a significant increase and are consistent with the range reported for Spanish groundwater, which varies from 1.4 to 78 Bq·m^{-3} (average 20 ± 7 Bq·m^{-3}) (Pérez-Moreno et al., 2020). Our results also agree well with the ^{210}Pb values reported for slightly contaminated groundwater in the uranium-mineralized area of Jaduguda, India, which average 9.3 ± 2.1 Bq·m^{-3} (Sharma et al., 2021). In contrast, other regions affected by uranium mining exhibit much higher ^{210}Pb levels (e.g. Dias da Cunha et al., 2014). The higher activity values found in one of the aliquots (18 ± 2 Bq·m^{-3}) might correspond to particulate material or precipitate present in the unfiltered water that prevented all the aliquots to be totally homogeneous.

For coastal surface seawater, the determined ^{210}Po activities show good agreement between the samples collected in the Gulf of Cádiz, Huelva and Cádiz, (Batches D and E, respectively). These values also fall within the range reported in the literature for ^{210}Po in coastal surface waters, from 0.25 to 3.39 Bq·m^{-3} (Chung & Wu, 2005; Gascó et al., 2002; Gasco & Anton, 1999.; Masqué et al., 2002; Meli et al., 2011, 2013). Specifically, they agree with previously reported values for the southern Atlantic coast: 0.50–1.94 Bq·m^{-3} (Gascó et al., 2002) and 0.47–1.7 Bq·m^{-3} (Gascó & Antón, 1999).

4.1.2. Open ocean samples from PAP cruises

To validate the Fe^{2+} method, it was applied to open-ocean samples collected during NOC and APERO cruises (Figures 1 and 2). Determined ^{210}Po and ^{210}Pb activity concentrations during both cruises agree well with those reported from previous PAP-site studies, 0.45 – 2.1 Bq·m^{-3} for ^{210}Po and 1.06 – 6.7 Bq·m^{-3} for ^{210}Pb (Horowitz et al., 2020; Le Moigne et al., 2013; Tang & Stewart, 2019).

Both ^{210}Po and ^{210}Pb radioisotopes show the expected biogeochemically behaviour in the seawater column. In the EZ, ^{210}Po deficits relative to ^{210}Pb (^{210}Po/^{210}Pb <1) are due to ^{210}Po being preferentially scavenged by sinking particulate matter (Chung & Finkel, 1988). Whereas ^{210}Pb is only adsorbed on particles surface, ^{210}Po is strongly adsorbed on particles, but also incorporated to the phytoplankton cells, and bioaccumulated through the food web (Cherrier et al., 1995; Larock et al., 1996; G. M. Stewart & Fisher, 2003).

In the TZ, the obtained ^{210}Po/^{210}Pb ratios were closer to 1 due to the absence of net removal or ^{210}Po addition occurring faster than their ingrowth–decay (e.g. Roca-Martí & Puigcorbé, 2024). Profiles SS1, SS2 and SS3 show ^{210}Po excess values in relation to ^{210}Pb (^{210}Po/^{210}Pb > 1) from 250 m downward that likely reflects the release of particulate ^{210}Po to non-sinking phases through remineralization or disaggregation processes carried out mainly by bacteria and zooplankton (e.g.Villa-Alfageme et al., 2014).

Determined ^{210}Po and ^{210}Pb activity concentrations during both cruises agree well with those reported from previous PAP-site studies, 0.45–2.1 Bq·m^{-3} for ^{210}Po and 1.06–6.7 Bq·m^{-3} for ^{210}Pb (Horowitz et al., 2020; Le Moigne et al., 2013; Tang & Stewart, 2019). It is noteworthy the remarkable agreement, found in the profiles SS1-SS5 from the APERO cruise, between POC and ^{210}Po fluxes obtained from ^{210}Po–^{210}Pb disequilibrium and those obtained from sediment traps (López Rodríguez et al., 2025; López Rodríguez et al., in prep). This strong agreement within methods validates the use of Fe^{2+} as an alternative method for ^{210}Po and ^{210}Pb measurements.

Our results in the water column also align well with those reported by Tang et al., (2018), who presented ^{210}Po – ^{210}Pb depth profiles along a North Atlantic transect during the GEOVIDE program. Two of their sampled stations were located near the PAP Site (Stations 21 and 26; see Figure 1 in the article). Figure S2 shows average ^{210}Po–^{210}Pb activities obtained during the NOC and APERO campaigns and those from GEOVIDE. In addition to the good agreement observed in the range of measured values for ^{210}Po and ^{210}Pb, both radioisotopes show similar vertical patterns in the water column: ^{210}Po deficits in the EZ (~ 50 m) due to particle scavenging, and either secular equilibrium or ^{210}Po excesses below ~250 m in the TZ.

In Tang et al., (2018), the Co-APDC coprecipitation method was applied to determine ^{210}Po and ^{210}Pb activities. This method has proven highly effective and robust for isolating ^{210}Po from seawater in numerous oceanographic campaigns (e.g., Gascó et al., 2002; Moore & Smith, 1986; Robert, 1997.; Roca-Martí et al., 2016, 2021a; Smith et al., 2003; Tang et al., 2018). As a main disadvantage, this method requires the individual filtration

of every sample after coprecipitation of polonium with the insoluble Co-APDC chelate (Fleer & Bacon, 1984), making the method labour-intensive and time-consuming on board.

In contrast, the Fe^{2+} method allows the precipitate to be easily recovered by siphoning the supernatant, which is particularly relevant during oceanographic cruises. The coprecipitation step is usually performed on board immediately after sampling, minimizing the elapsed time to ^{210}Po determination and preventing ^{210}Po decay from biasing the original ^{210}Po – ^{210}Pb disequilibrium at the sampling date. Since large seawater volumes are processed at multiple stations with limited time between casts, the coprecipitation method must be as simple and efficient as possible for shipboard application.

In addition to its application for the determination of ^{210}Po in fresh water matrices (Waples, 2020; Waples et al., 2025), the Fe^{2+} coprecipitation method has also been successfully applied to extract and measure ^{237}Np and ^{236}U in seawater matrices (Chamizo et al., 2016; López-Lora et al., 2019, 2020), as well as in numerous previous studies to remove toxic metalloids such as arsenic and bismuth from various water matrices, being more effective in removing them than Fe^{3+} (Ciardelli et al., 2008; Muñiz et al., 2009; Sahai et al., 2007; Xu et al., 2022).

4.2. Performance of Fe^{2+} vs Fe^{3+} coprecipitation methods

The Fe^{3+} coprecipitation method was already applied in the 60s (e.g. Bath et al., 1969), and currently is the most widely used technique for determining ^{210}Po in seawater. However, there is extensive literature reporting analytical problems in the measurement of ^{210}Po and its disequilibrium in depth with ^{210}Pb with this method (Roca-Martí et al., 2021).

Three groups were the first to report problems in the measurement of ^{210}Po and ^{210}Pb in seawater samples during the GEOSECS program. Chung & Craig (1983) found a systematic underestimation of ^{210}Pb using the Fe^{3+} method by about 30%. Cochran et al., (1983) reported ^{210}Po deficiencies relative to ^{210}Pb in the TZ, which were not observed when applying the Co-APDC method.

Unexpected ^{210}Po deficits observed in even deeper waters (up to 3000 m) were also reported in the intercalibration exercise conducted during the GEOTRACES program (Church et al., 2012), as well as in numerous other campaigns which applied the Fe^{3+} method (Ceballos-Romero et al., 2016; Kim, 2001.; Kim et al., 1999; Rigaud et al., 2015; Roca-Martí et al., 2021). The recent study Roca-Martí et al., (2021) reported that, among the 213 depth profiles analysed, ^{210}Po – ^{210}Pb disequilibrium at depths > 300 m occurred in twice as many profiles when using the Fe^{3+} method compared with Co-APDC. In addition, they found that the Fe^{3+} method systematically underestimated ^{210}Po activity concentrations by an average of 35%.

Interestingly, measurement problems with the Fe^{3+} method are not limited to ^{210}Po and ^{210}Pb, López-Lora et al., (2018) also reported low chemical yields for uranium extraction during ^{236}U evaluation from seawater samples when using this method.

4.2.1. Underestimation of ^{210}Po activities

In addition to testing and validating the performance of Fe^{2+} method in different water matrices, we collected replicates, which were processed and measured using the Fe^{3+} method. The comparison of replicate results relative to the Fe^{2+} method is presented in Figures 2 and 3. Both the systematic ^{210}Po activity underestimation and deep ^{210}Po deficits when using the Fe^{3+} method are also evident in this study.

Figure 3 compares the ^{210}Po activity concentrations determined in all replicate samples processed using the Fe^{3+} and Fe^{2+} coprecipitation methods. These results include groundwater and coastal seawater samples from southern Spain (Figure S1), as well as the open-ocean water samples collected during the two sampling campaigns conducted around the PAP site (Figure 1). The complete dataset can be found in Table 1.

Within uncertainties, Fe^{3+} method underestimates ^{210}Po activity in 23 out of 42 replicates from all water matrices analysed in this work. In 18 replicates both methods yield the same activity, and only in 1 replicate the Fe^{2+} method underestimates ^{210}Po activity.

In the coastal surface seawater samples, ^{210}Po activities of Fe^{2+} and Fe^{3+} agreed within uncertainties in 6 out of 10 replicates. In the remaining 4 replicates, the Fe^{2+} method yielded higher activities ranging from 33 – 52 % (averaging 41 ± 6 %) relative to the Fe^{3+} method.

Among the 24 analysed open-ocean sample replicates, the Fe^{3+} method yielded a higher ^{210}Po activity in only one replicate, by 29 ± 11 %. In five replicates, both methods measured the same ^{210}Po activity. In the remaining 18 replicates, the Fe^{2+} method consistently yielded higher ^{210}Po activities, with differences ranging from 17% to 78%, averaging 42 ± 18 %.

It is noteworthy that the systematic ^{210}Po underestimation activities determined from the open - ocean samples from PAP cruises are depth independent, as shown in the zoomed view of Figure 3. Indeed, average ^{210}Po underestimation with the Fe^{3+} method relative to Fe^{2+} is 40 ± 8 % in the EZ and 37 ± 5 % in the TZ. This consistency in the results indicates that the observed underestimation is not related to replicate bias or to depth-dependent biological or biogeochemical processes occurring within the water column but rather reflects a methodological bias inherent to the Fe^{3+} approach.

Regarding ^{210}Pb activities, determined range values are similar for the two methods in all sampled stations. Average ^{210}Pb was 1.5 ± 0.3 Bq $\cdot m^{-3}$ for Fe^{2+} and 1.3 ± 0.4 Bq $\cdot m^{-3}$ for Fe^{3+} in both NOC and APERO cruises.

Differences within methods are similar and pronounced in coastal surface and open-ocean samples. In both water matrices, ^{210}Po activities are, on average, 42 ± 10 % higher when

using the Fe^{2+} method compared with Fe^{3+}. This is very similar to the average ^{210}Po underestimation of 35% reported by Roca-Martí et al., (2021) in replicates processed with Fe^{3+} relative to the Co-APDC method.

In contrast, we observed very small differences between the two methods in the groundwater samples, where the results cluster near the 1:1 line (Figure 3). Within uncertainties, ^{210}Po activities were equal between the two methods in eight out of nine processed replicates. Only in a single replicate, the ^{210}Po activity determined with the Fe^{2+} method was 43 ± 13 % higher than that obtained using the Fe^{3+} method. Average ^{210}Po values were equal in Batches A and C, whereas in Batch B, ^{210}Po activity was higher with the Fe^{2+} method by 32 ± 6 %. These results are consistent with those reported by Waples et al., (2025), who found no differences in the determined ^{210}Po by comparing the three Fe^{2+}, Fe^{3+} and Co-APDC coprecipitation methods in several natural water replicates. The difference in these fresh samples in relation to seawater sample is not only the origin of the water, but also that groundwater were stored and acidified for more than one year, allowing the salts and organic phases to dissolve and degrade into simpler compounds.

4.2.2. ^{210}Po and ^{210}Pb seawater profiles

Figure 2 also includes in dashed lines the ^{210}Pb – ^{210}Pb depth profiles obtained by applying the Fe^{3+} method in the replicates collected from both NOC and APERO cruises (See data in Table S1). As discussed above, the Fe^{3+} method systematically underestimates ^{210}Po activity throughout the water column. This fact has important implications for the interpretation of ^{210}Pb - ^{210}Po depth profiles.

As noted earlier, ^{210}Po deficits in the EZ are due to its preferential scavenging relative to ^{210}Pb onto sinking organic matter (Villa-Alfageme et al., 2014). Although these deficits are observed using both methods, the Fe^{3+} method overestimates the ^{210}Pb – ^{210}Po disequilibrium relative to the Fe^{2+} method by 15 – 65% (averaging 34 ± 22 %) in the EZ.

In the TZ, when export events no longer take place, both radioisotopes are expected to reach secular equilibrium (Ceballos-Romero et al., 2016). However, the Fe^{3+} method also overestimates the ^{210}Pb – ^{210}Po disequilibrium in this region, even more than in the EZ, with values ranging from 10 - 74 % (averaging 43 ± 25 %). This overestimation prevents both radioisotopes from reaching secular equilibrium at depths at which it is reached with the Fe^{2+} method.

Indeed, both radioisotopes reach secular equilibrium in the TZ with the Fe^{2+} method at all stations, with average $^{210}Po/^{210}Pb$ ratios ranging from 0.9 - 1.1 (averaging 1.1 ± 0.3), except at SS3, where the elevated mean of 1.6 ± 0.4 is likely due to intense remineralization processes carried out by bacterial communities (Gesson et al., 2025). On the other hand, ^{210}Po underestimation using the Fe^{3+} method deviates both radionuclides from equilibrium in the TZ using this method, with $^{210}Po/^{210}Pb$ ratios ranging from 0.49 to 0.99 (averaging 0.80 ± 0.20).

More specifically, at station SS1-1, both radioisotopes consistently reach secular equilibrium throughout the TZ when using the Fe^{2+} method, whereas this equilibrium is disrupted by large ^{210}Po deficits within the TZ at 150 and 400 m when using Fe^{3+}. A similar pattern is observed at most stations sampled during the APERO cruises: at stations SS3 and SS5, secular equilibrium along the TZ is observed only with the Fe^{2+} method and is not achieved with Fe^{3+} due to ^{210}Po deficits. At station SS4 both methods yield a consistent secular equilibrium at most depths in the TZ.

Thus, ^{210}Po underestimation using the Fe^{3+} vs Fe^{2+} methods leads to a more unvarying secular equilibrium below the export zone between both radioisotopes when the Fe^{2+} method is employed, while it is disrupted in the TZ with Fe^{3+}.

In the literature, ^{210}Po deficits, and thus ^{210}Po-^{210}Pb disequilibrium in deep waters, are typically explained from the unequal adsorption and desorption processes affecting sinking particulate matter (De Soto et al., 2018), or to ^{210}Po being scavenged in unorthodox ways by deepen phytoplankton (Chung & Wu, 2005; Church et al., 2012; Cochran et al., 1983; Wei et al., 2014). In this study, we find that such deep ^{210}Po deficits occur more frequently when the Fe^{3+} method is employed compared to Fe^{2+}. Similarly, Roca-Martí et al., (2021) reported more consistent equilibrium between both radioisotopes when using the Co-APDC method relative to the Fe^{3+} method.

4.3. Improvements of using Fe^{2+} over Fe^{3+} for polonium coprecipitation

Both Fe^{3+} and Fe^{2+} methods yielded high and very similar chemical yields across all analysed water matrices, averaging 52 ± 10 % for Fe^{3+} and 50 ± 10 % for Fe^{2+}. These chemical yields also align with those reported in the literature, ranging from 40 – 87 % in groundwater samples (Bonotto et al., 2009; Idoeta et al., 2011; Ruberu et al., 2007; Vesterbacka & Ikäheimonen, 2005) and from 20 – 71 % in seawater (Kawakami et al., 2014; Le Moigne et al., 2013; Thakur & Ward, 2020; Villa-Alfageme et al., 2014, 2024; Zhong et al., 2020)

The results of this study, along with those from the abovementioned literature indicate that the Fe^{3+} method systematically overestimates ^{210}Po – ^{210}Pb disequilibrium throughout the water column, and therefore the downward POC fluxes. As, the ^{210}Pb – ^{210}Po disequilibrium is a widely employed approach to estimate POC fluxes (Le Moigne et al., 2013) and any potential bias in the measurement of these radioisotope activities directly affects the accuracy of the estimated sinking POC (Church et al., 2012).

There are different reasons that account for the observed ^{210}Po deficits measured using the Fe^{3+}method. According to equation (2), ^{210}Po activity is determined from the count-rate ratio of ^{210}Po to ^{209}Po, multiplied by the known activity of ^{209}Po (Rigaud et al., 2013; Roca-Martí et al., 2021). This equation assumes that ^{210}Po and ^{209}Po are chemically equivalent, and recovered in the same proportion (i.e., with the same chemical yield) during the polonium isolation step (Section 2.2.). However, as it is suggested by Church et al., (2012), obtaining the same extraction of ^{210}Po and ^{209}Po strongly depends on the

coprecipitation method applied. The unequal extraction of both ^{210}Po and ^{209}Po could explain the underestimation of ^{210}Po activity observed with the Fe^{3+} method in the analysed replicates If ^{209}Po were not efficiently recovered and reported, in relation to ^{210}Po, during the radiochemical method, the ^{210}Po results would be overestimated. Therefore, this hypothesis is ruled out, as the results clearly show an underestimation of ^{210}Po.

Therefore, the underestimation of ^{210}Po with Fe^{3+} could be due to either a deficient extraction of ^{210}Po relative to ^{209}Po or, conversely, to an overestimation of ^{209}Po. The latter overestimation would be originated by a systematic contamination during the radiochemical separation; however, the blanks prepared for the different baches do not show any additional contribution of ^{209}Po. The second hypothesis considers that the spike ^{209}Po is correctly coprecipitated, but ^{210}Po is not recovered in the same proportion. This explanation was first proposed by Church et al., (2012) and later supported by the results of Nowicki et al., (2022) and Roca-Martí et al., (2021). The time available on the ship between the sample pre-conditioning and the coprecipitation method is about 8 hours. During this time, the speciation of both radioisotopes, ^{210}Po and ^{209}Po, may not be homogeneous. Because while ^{209}Po is added a few hours before the coprecipitation, ^{210}Po is strongly bound to organic matter (Stewart et al., 2007); as a result, ^{210}Po would be disenclined to be extracted and may be recovered in lower proportion than the ^{209}Po tracer. The results reported in Ma et al., (2021) supports this hypothesis, they obtained a consistent secular equilibrium between ^{210}Po and ^{210}Pb throughout the entire TZ. The Fe^{3+} method was applied, with the distinction that the elapsed time between sampling and the coprecipitation step was ~ 50 days. This period would be enough for the formation of free natural ^{210}Po radicals, which can then be efficiently extracted along with the ^{209}Po spike by the carrier.

Similar results are obtained in groundwater samples measurements. The elapsed time between collection and coprecipitation was at least one year in all the groundwater samples. In the meantime, they were stored acidified with nitric acid, allowing the acid to attack and break down the organic compounds and dissolve the salt present in the seawater. Allowing to form free ^{210}Po radicals that can be more easily extracted during the coprecipitation, together with the tracer.

This unequal and not easily traceable extraction of ^{210}Po and ^{209}Po would be more significant in seawater than in groundwater samples, as seawater are more complex matrices due to their high salt and organic matter content (Villa-Alfageme et al., 2016). Accordingly, Waples et al., (2025) recently showed non-significant bias between the Fe^{3+}, Fe^{2+} and Co-APDC methods in natural water matrices. This is consistent with our results: both Fe^{3+} and Fe^{2+} methods yielded similar ^{210}Po activities in most groundwater replicates, likely because in these matrices both methods extract ^{209}Po and ^{210}Po correctly and in an equal proportion.

It is important noting that the inefficient extraction of radioisotopes from seawater using coprecipitation with Fe^{3+} is not specific to polonium López-Lora et al., (2018) reported

average chemical yields of 52 ± 25 % for ^{236}U extraction using the Fe^{3+} method, which increased to 93 ± 8 % when using Fe^{2+} (López-Lora et al., 2019). And for the ^{237}Np the chemical yield using Fe^{3+} is negligible, versus using coprecipitation with Fe^{2+}, where the chemical yield increases up to 87 ± 6 % (López-Lora et al., 2019).

In summary, the results of our study, along with those reported by (López-Lora et al., 2018, 2019; Roca-Martí et al., 2021) indicate that the Fe^{2+}, Fe^{3+}, and Co-APDC methods speciate actinides and ^{210}Po differently in seawater. When ^{210}Po is extracted from the seawater matrix, the spiked ^{209}Po is not sensitive to these differences in speciation using the three different methods, as it is usually added only before the radiochemical analysis. The Fe^{2+} and Co-APDC approaches likely produce a similar speciation of natural ^{210}Po in seawater, which is extracted in the same proportion relative to ^{209}Po by both methods. The alignment within methods reported by Waples et al., (2025) in freshwater suggests that this effect may only concern seawater matrices; in freshwater, natural ^{210}Po may be similarly speciated by the three methods, subsequently leading to consistent analytical results.

Finally, it is important to note that there is not much available research regarding the speciation of polonium in water samples; for this reason, it is necessary to further analyse and quantify how the intrinsic properties of the Fe^{2+} and Fe^{3+} precipitants influence the accuracy of the results. It is known that differences in ionic radius and charge, as well as factors such as pH, ionic strength, and the presence of complexing agents affect the coprecipitation of polonium by influencing its speciation and interactions with the precipitate surface (Cerrahoğlu et al., 2017; Xu et al., 2022; Yang et al., 2022).

5. Summary and Conclusions

In this study, we set up a novel method to determine ^{210}Po and ^{210}Pb in seawater, based on the coprecipitation of ^{210}Po and ^{209}Po with Fe^{2+}. The performance of the new method has been developed using different water matrices, including fresh groundwater, coastal seawater and open ocean samples, with chemical yields ranging from 31 - 68%, with an average of 46 ± 9 %. The method yielded ^{210}Po and ^{210}Pb activities that align well with previously reported values in the literature for the different water matrices analysed.

The method was applied to the measurement of ^{210}Po and ^{210}Pb depth profiles in open ocean during two oceanographic cruises. The two radioisotopes showed activity concentration patterns through the water column describing a ^{210}Po-^{210}Pb disequilibrium in the upper water column, in the productive euphotic zone, associated to the ^{210}Po scavenging by downward organic sinking particles; and a subsequent ^{210}Po-^{210}Pb equilibrium below the euphotic zone where the production and sinking of particles is negligible. Specific profiles showed and increasing of ^{210}Po over ^{210}Pb below the euphotic zone due to remineralization and fragmentation of the sinking particles.

Replicates were collected for the three different matrices and processed using the traditional method based on Fe^{3+} coprecipitation. ^{210}Po and ^{210}Pb depth profiles measured

using Fe^{3+} coprecipitation were measured in open ocean and a persistent disequilibrium ^{210}Po-^{210}Pb below the euphotic zone, not associated to depths with negligible ^{210}Po scavenging, it is found. This result points out to an underestimation of ^{210}Po using this method.

When the results from both methods, based on Fe^{2+} and Fe^{3+} coprecipitation, were compared in the three matrices, the Fe^{3+} method underestimates ^{210}Po activities by an average of 41 ± 6 % relative to Fe^{2+} in the coastal surface and open-ocean replicate samples. This underestimation is consistent with the 35 % reported by Roca-Martí et al., (2021) when comparing the Co-APDC and Fe^{3+} methods in open-ocean waters. However, no significant differences between methods were observed in the groundwater replicates.

The systematic ^{210}Po underestimation observed when using the polonium Fe^{3+} coprecipitation along the entire water column in the open-ocean depth profiles, that prevents ^{210}Po and ^{210}Pb from reaching secular equilibrium directly influences the accuracy with which downward POC fluxes are determined using the proxy based on ^{210}Pb – ^{210}Po disequilibrium. The secular equilibrium ^{210}Pb – ^{210}Po is consistently achieved using a coprecipitation based on Fe^{2+}. Furthermore, during our sampling cruises it was found that POC fluxes derived from the Fe^{2+} method strongly agree with those measured using alternative methods such as sediment traps. Overall, these results support the importance of developing a rigorous coprecipitation of polonium, especially in seawater, suggesting a coprecipitation based on Fe^{2+}, instead of Fe^{3+}.

ACKNOWLEDGMENTS AND FINANTIAL SUPPORT:

We thank the captain and crew of the RSS Discovery during JC231 for their help during mobilisation. We acknowledge the use of the Sea of Thorium compilation and the Ocean Productivity database from Oregon State University, which provided essential data for this study.

This work has been funded by the SPOCK project (PID2023-149513NB-I00), supported by Plan Estatal 2021-2023. A. López-Rodríguez and B. González-González have been funded by Project Grant: DEPOCARBON (No. PCM00063), “Planes Complementarios con las Comunidades Autónomas”. Plan de Recuperacion de Transformacion y Resiliencia (PRTR) and Plan Complementario de I+D+I.

This Article contributes to the APERO project funded by the National Research Agency under the grant APERO (grant no. ANR ANR- 21-CE01-0027) lead by Laurent Memery, Christian Tamburini and Lionel Guidi, and by the French LEFE-Cyber programme (CNRS, INSU). The authors thank Christian Tamburini (Chief scientist), the captain and crew of N/O ‘Le Pourquoi Pas’ (Flotte Océanographique Française) for their help during the APERO cruise (https://doi.org/10.17600/1800066). We thank the ‘Moyen Commun’ SAM and Radioactivity from the Mediterranean Institute of Oceanography (MIO) as well as the ‘parc national d’instrumentation océanographique’ (PNIO) of the ‘division technique de l’Institut national des sciences de l’Univers du CNRS (DT INSU) for their

technical expertise and facilities. This work was also supported by ANR-JC ARMORIC-ANR-21 CE01-0005 granted to F.L.M.

References

Bath et al. (1969). *234Th/238U Ratios in the Ocean*. https://doi.org/10.1016/S0012-821X(68)80083-4

Bonotto, D. M., Caprioglio, L., Bueno, T. O., & Lazarindo, J. R. (2009). Dissolved 210Po and 210Pb in Guarani aquifer groundwater, Brazil. *Radiation Measurements*, *44*(3), 311–324. https://doi.org/10.1016/j.radmeas.2009.03.022

Boyd, P. W., Claustre, H., Levy, M., Siegel, D. A., & Weber, T. (2019). Multi-faceted particle pumps drive carbon sequestration in the ocean. In *Nature* (Vol. 568, Number 7752, pp. 327–335). Nature Publishing Group. https://doi.org/10.1038/s41586-019-1098-2

Buesseler, K. O., Boyd, P. W., Black, E. E., Siegel, D. A., Designed, D. A. S., & Performed, E. E. B. (2020). *Metrics that matter for assessing the ocean biological carbon pump*. https://doi.org/10.1073/pnas.1918114117/-/DCSupplemental

Ceballos-Romero, E., Le Moigne, F. A. C., Henson, S., Marsay, C. M., Sanders, R. J., García-Tenorio, R., & Villa-Alfageme, M. (2016). Influence of bloom dynamics on Particle Export Efficiency in the North Atlantic: a comparative study of radioanalytical techniques and sediment traps. *Marine Chemistry*, *186*, 198–210. https://doi.org/10.1016/j.marchem.2016.10.001

Cerrahoğlu, E., Kayan, A., & Bingöl, D. (2017). New Inorganic–Organic Hybrid Materials and Their Oxides for Removal of Heavy Metal Ions: Response Surface Methodology Approach. *Journal of Inorganic and Organometallic Polymers and Materials*, *27*(2), 427–435. https://doi.org/10.1007/s10904-016-0483-7

Chamizo, E., López-Lora, M., Bressac, M., Levy, I., & Pham, M. K. (2016). Excess of 236U in the northwest Mediterranean Sea. *Science of the Total Environment*, *565*, 767–776. https://doi.org/10.1016/j.scitotenv.2016.04.142

Cherrier, J., Burnett, W. C., & LaRock, P. A. (1995). Uptake of polonium and sulfur by bacteria. *Geomicrobiology Journal*, *13*(2), 103–115. https://doi.org/10.1080/01490459509378009

Chung, Y., & Craig, H. (1983). 21°pb in the Pacific: the GEOSECS measurements of particulate and dissolved concentrations. In *406 Earth and Planetary Science Letters* (Vol. 65). Elsevier Science Publishers B.V.

Chung, Y., & Finkel, R. (1988). 21°po in the western Indian Ocean: distributions, disequilibria and partitioning between the dissolved and particulate phases. In *Earth and Planetary Science Letters* (Vol. 88). Elsevier Science Publishers B.V.

Chung, Y., & Wu, T. (2005). Large 210Po deficiency in the northern South China Sea. *Continental Shelf Research*, *25*(10), 1209–1224. https://doi.org/10.1016/j.csr.2004.12.016

Church, T., Rigaud, S., Baskaran, M., Kumar, A., Friedrich, J., Masque, P., Puigcorbé, V., Kim, G., Radakovitch, O., Hong, G., Choi, H., & Stewart, G. (2012). Intercalibration studies of 210Po and 210Pb in dissolved and particulate seawater samples. *Limnology and Oceanography: Methods*, *10*(OCTOBER), 776–789. https://doi.org/10.4319/lom.2012.10.776

Ciardelli, M. C., Xu, H., & Sahai, N. (2008). Role of Fe(II), phosphate, silicate, sulfate, and carbonate in arsenic uptake by coprecipitation in synthetic and natural groundwater. *Water Research*, *42*(3), 615–624. https://doi.org/10.1016/j.watres.2007.08.011

Cochran, J. K., Bacon, M. P., Krishnaswami, S., & Turekian, K. K. (1983). 21°po and 21°pb distributions in the central and eastern Indian Ocean. In *Earth and Planetary Science Letters* (Vol. 65).

De Soto, F., Ceballos-Romero, E., & Villa-Alfageme, M. (2018). A microscopic simulation of particle flux in ocean waters: Application to radioactive pair disequilibrium. *Geochimica et Cosmochimica Acta*, *239*, 136–158. https://doi.org/10.1016/j.gca.2018.07.031

Dias da Cunha, K. M., Henderson, H., Thomson, B. M., & Hecht, A. A. (2014). Ground water contamination with 238U, 234U, 235U, 226Ra and 210Pb from past uranium mining: Cove wash, Arizona. *Environmental Geochemistry and Health*, *36*(3), 477–487. https://doi.org/10.1007/s10653-013-9575-2

Fleer, A. P., & Bacon, M. P. (1984). Determination of 210Pb and 210Po in seawater and marine particulate matter. In *Nuclear Instruments and Methods in Physics Research* (Vol. 223).

Gasco, C., & Anton, M. P. (1999). *IAEA-SM-354/260P XA9952092 Plutonium and polonium concentrations in the different water masses crossing the strait of Gibraltar*.

Gascó, C., Antón, M. P., Delfanti, R., González, A. M., Meral, J., & Papucci, C. (2002). Variation of the activity concentrations and fluxes of natural (210 Po, 210 Pb) and anthropogenic (239,240 Pu, 137 Cs) radionuclides in the Strait of Gibraltar (Spain). In *Journal of Environmental Radioactivity* (Vol. 62). www.elsevier.com/locate/jenvrad

Gesson, M., C Le Moigne, F. A., & Villa Alfageme, M. (2025). *Particle flux attenuation in Northeast Atlantic during APERO*.

Giering, S. L. C., Sanders, R., Lampitt, R. S., Anderson, T. R., Tamburini, C., Boutrif, M., Zubkov, M. V., Marsay, C. M., Henson, S. A., Saw, K., Cook, K., & Mayor, D. J. (2014). Reconciliation of the carbon budget in the ocean's twilight zone. *Nature*, *507*(7493), 480–483. https://doi.org/10.1038/nature13123

Hartman, S. E., Bett, B. J., Durden, J. M., Henson, S. A., Iversen, M., Jeffreys, R. M., Horton, T., Lampitt, R., & Gates, A. R. (2021). Enduring science: Three decades of observing the Northeast Atlantic from the Porcupine Abyssal Plain Sustained Observatory (PAP-SO). *Progress in Oceanography*, *191*. https://doi.org/10.1016/j.pocean.2020.102508

Henson, S., Laufkötter, C., Leung, S., Giering, S., Palevsky, H., & Cavan, E. (2022). *What the flux? Uncertain response of ocean biological carbon export in a changing world*. https://doi.org/10.1002/essoar.10507873/v3

Horowitz, E. J., Cochran, J. K., Bacon, M. P., & Hirschberg, D. J. (2020). 210Po and 210Pb distributions during a phytoplankton bloom in the North Atlantic: Implications for POC export. *Deep-Sea Research Part I: Oceanographic Research Papers*, *164*. https://doi.org/10.1016/j.dsr.2020.103339

Idoeta, R., Herranz, M., & Legarda, F. (2011). The disequilibrium between 210Po and 210Pb in raw and drinking waters. *Applied Radiation and Isotopes*, *69*(1), 196–200. https://doi.org/10.1016/j.apradiso.2010.07.021

Katzlberger, C., Wallner, G., & Irlweck, K. (2001). Determination of 210 Pb, 210 Bi and 210 Po in natural drinking water. In *Journal of Radioanalytical and Nuclear Chemistry* (Vol. 249, Number 1).

Kawakami, H., Honda, M. C., Watanabe, S., & Sino, T. (2014). Time-series observations of 210Po and 210Pb radioactivity in the western North Pacific. *Journal of Radioanalytical and Nuclear Chemistry*, *301*(2), 461–468. https://doi.org/10.1007/s10967-014-3141-y

Kim, G. (2001). *Large de¢ciency of polonium in the oligotrophic ocean's interior*. www.elsevier.com/locate/epsl

Kim, G., Hussain, N., Church, T. M., & Yang, H.-S. (1999). A practical and accurate method for the determination of 234 Th simultaneously with 210 Po and 210 Pb in seawater. In *Talanta* (Vol. 49).

Kimberly A. Roberts, Cochran, J. K., & Barnes Christina. (1996). *210Pb and 239,240Pu in the Northeast Water Polynya, Greenland: particle dynamics and sediment mixing rates*.

Larock, P., Hyun, J.-H., Boutelle, L. S., Burnett, W. C., & Hull, C. D. (1996). Bacterial mobilization of polonium. In *Geochimica et Cosmochimica Acta* (Vol. 60, Number 22).

Le Moigne, F. A. C. (2019). Pathways of Organic Carbon Downward Transport by the Oceanic Biological Carbon Pump. In *Frontiers in Marine Science* (Vol. 6). Frontiers Media S.A. https://doi.org/10.3389/fmars.2019.00634

Le Moigne, F. A. C., Villa-Alfageme, M., Sanders, R. J., Marsay, C., Henson, S., & García-Tenorio, R. (2013). Export of organic carbon and biominerals derived from 234Th and 210Po at the Porcupine Abyssal Plain. *Deep-Sea Research Part I: Oceanographic Research Papers*, *72*, 88–101. https://doi.org/10.1016/j.dsr.2012.10.010

López Rodríguez, Á., González González, B., Hurtado Bermúdez, S., Le Moigne, F., Gesson, M., & Villa Alfageme, M. (2025). *Analysis of Export and Transfer Efficiency around the PAP-Site Observatory: an update from the APERO project*. https://doi.org/10.5194/egusphere-egu25-13345

López-Lora, M., Chamizo, E., Rožmarić, M., & Louw, D. C. (2020). Presence of 236U and 237Np in a marine ecosystem: The northern Benguela Upwelling System, a case study. *Science of the Total Environment*, *708*. https://doi.org/10.1016/j.scitotenv.2019.135222

López-Lora, M., Chamizo, E., Villa-Alfageme, M., Hurtado-Bermúdez, S., Casacuberta, N., & García-León, M. (2018). Isolation of 236U and 239,240Pu from seawater samples and its determination by Accelerator Mass Spectrometry. *Talanta*, *178*, 202–210. https://doi.org/10.1016/j.talanta.2017.09.026

López-Lora, M., Levy, I., & Chamizo, E. (2019). Simple and fast method for the analysis of 236U, 237Np, 239Pu and 240Pu from seawater samples by Accelerator Mass Spectrometry. *Talanta*, *200*, 22–30. https://doi.org/10.1016/j.talanta.2019.03.036

Ma, Q., Qiu, Y., Zhang, R., Lv, E., Huang, Y., & Chen, M. (2021). 210Po/210Pb Disequilibria in the Eastern Tropical North Pacific. *Frontiers in Marine Science*, *8*. https://doi.org/10.3389/fmars.2021.716688

Marra, J. F., Lance, V. P., Vaillancourt, R. D., & Hargreaves, B. R. (2014). Resolving the ocean's euphotic zone. *Deep-Sea Research Part I: Oceanographic Research Papers*, *83*, 45–50. https://doi.org/10.1016/j.dsr.2013.09.005

Masqué, P., Sanchez-Cabeza, J. A., Bruach, J. M., Palacios, E., & Canals, M. (2002). Balance and residence times of 210 Pb and 210 Po in surface waters of the northwestern Mediterranean Sea. In *Continental Shelf Research* (Vol. 22).

Matthews, K. M., Kim, C. K., & Martin, P. (2007). Determination of 210Po in environmental materials: A review of analytical methodology. In *Applied Radiation and Isotopes* (Vol. 65, Number 3, pp. 267–279). https://doi.org/10.1016/j.apradiso.2006.09.005

Meli, M. A., Desideri, D., Penna, A., Ricci, F., & Roselli, C. (2013). 210 Po and 210 Pb Concentration in Environmental Samples of the Adriatic Sea. *Int. J. Environ. Res*, *7*(1), 51–60.

Meli, M. A., Desideri, D., Roselli, C., & Feduzi, L. (2011). Analytical methods to determine 210Po and 210Pb in marine samples. *Microchemical Journal*, *99*(2), 273–277. https://doi.org/10.1016/j.microc.2011.05.013

Moore, R. M., & Smith, J. N. (1986). Disequilibria between 226 Ra, 210 Pb and 210 Po in the Arctic Ocean and the implications for chemical modification of the Pacific water inflow. In *Earth and Planetary Science Letters* (Vol. 77).

Muñiz, G., Fierro, V., Celzard, A., Furdin, G., Gonzalez-Sánchez, G., & Ballinas, M. L. (2009). Synthesis, characterization and performance in arsenic removal of iron-doped activated carbons prepared by impregnation with Fe(III) and Fe(II). *Journal of Hazardous Materials*, *165*(1–3), 893–902. https://doi.org/10.1016/j.jhazmat.2008.10.074

Nowicki, M., DeVries, T., & Siegel, D. A. (2022). Quantifying the Carbon Export and Sequestration Pathways of the Ocean's Biological Carbon Pump. *Global Biogeochemical Cycles*, *36*(3). https://doi.org/10.1029/2021GB007083

Pérez-Moreno, S. M., Guerrero, J. L., Mosqueda, F., Gázquez, M. J., & Bolívar, J. P. (2020). Hydrochemical behaviour of long-lived natural radionuclides in Spanish groundwaters. *Catena*, *191*. https://doi.org/10.1016/j.catena.2020.104558

Puigcorbé, V., Masqué, P., & Le Moigne, F. A. C. (2020). Global database of ratios of particulate organic carbon to thorium-234 in the ocean: improving estimates of the biological carbon pump. *Earth System Science Data*, *12*(2), 1267–1285. https://doi.org/10.5194/essd-12-1267-2020

Rigaud, S., Puigcorbé, V., Cámara-Mor, P., Casacuberta, N., Roca-Martí, M., Garcia-Orellana, J., Benitez-Nelson, C. R., Masqué, P., & Church, T. (2013). A methods assessment and recommendations for improving calculations and reducing uncertainties in the determination of 210Po and 210Pb activities in seawater. *Limnology and Oceanography: Methods*, *11*(OCT), 561–571. https://doi.org/10.4319/lom.2013.11.561

Rigaud, S., Stewart, G., Baskaran, M., Marsan, D., & Church, T. (2015). 210Po and 210Pb distribution, dissolved-particulate exchange rates, and particulate export along the North Atlantic US GEOTRACES GA03 section. *Deep-Sea*

Research Part II: Topical Studies in Oceanography, *116*, 60–78. https://doi.org/10.1016/j.dsr2.2014.11.003

Roca-Martí, M., & Puigcorbé, V. (2024a). *31:23 Annual Review of Marine Science Downloaded from www.annualreviews.org. Guest (guest) IP: 193.147.173.140 On: Fri*. https://doi.org/10.1146/annurev-marine-041923

Roca-Martí, M., & Puigcorbé, V. (2024b). *31:23 Annual Review of Marine Science Downloaded from www.annualreviews.org. Guest (guest) IP: 193.147.173.140 On: Fri*. https://doi.org/10.1146/annurev-marine-041923

Roca-Martí, M., Puigcorbé, V., Castrillejo, M., Casacuberta, N., Garcia-Orellana, J., Cochran, J. K., & Masqué, P. (2021). Quantifying 210Po/210Pb Disequilibrium in Seawater: A Comparison of Two Precipitation Methods With Differing Results. *Frontiers in Marine Science*, *8*. https://doi.org/10.3389/fmars.2021.684484

Roca-Martí, M., Puigcorbé, V., Rutgers van der Loeff, M. M., Katlein, C., Fernández-Méndez, M., Peeken, I., & Masqué, P. (2016). Carbon export fluxes and export efficiency in the central Arctic during the record sea-ice minimum in 2012: a joint 234Th/238U and 210Po/210Pb study. *Journal of Geophysical Research: Oceans*, *121*(7), 5030–5049. https://doi.org/10.1002/2016JC011816

Ruberu, S. R., Liu, Y.-G., & Perera, S. K. (2007). Ocurrence and distribution of 210Pb and 210Po in selected California groundwater wells. *Health Physics*. https://doi.org/10.1097/01.HP.0000254883.26386.9b

Sahai, N., Lee, Y. J., Xu, H., Ciardelli, M., & Gaillard, J. F. (2007). Role of Fe(II) and phosphate in arsenic uptake by coprecipitation. *Geochimica et Cosmochimica Acta*, *71*(13), 3193–3210. https://doi.org/10.1016/j.gca.2007.04.008

Sanders, R., Henson, S. A., Koski, M., De La Rocha, C. L., Painter, S. C., Poulton, A. J., Riley, J., Salihoglu, B., Visser, A., Yool, A., Bellerby, R., & Martin, A. P. (2014a). The Biological Carbon Pump in the North Atlantic. *Progress in Oceanography*, *129*(PB), 200–218. https://doi.org/10.1016/j.pocean.2014.05.005

Sanders, R., Henson, S. A., Koski, M., De La Rocha, C. L., Painter, S. C., Poulton, A. J., Riley, J., Salihoglu, B., Visser, A., Yool, A., Bellerby, R., & Martin, A. P. (2014b). The Biological Carbon Pump in the North Atlantic. *Progress in Oceanography*, *129*(PB), 200–218. https://doi.org/10.1016/j.pocean.2014.05.005

Sharma, D. B., Jha, V. N., Singh, S., Sethy, N. K., Sahoo, S. K., Jha, S. K., & Kulkarni, M. S. (2021). Distribution of 210Pb and 210Po in ground water around uranium mineralized area of Jaduguda, Jharkhand, India. *Journal of*

Radioanalytical and Nuclear Chemistry, *327*(1), 217–227. https://doi.org/10.1007/s10967-020-07495-w

Smith, J. N., Moran, S. B., & Macdonald, R. W. (2003). Shelf-basin interactions in the Arctic Ocean based on 210Pb and Ra isotope tracer distributions. *Deep-Sea Research Part I: Oceanographic Research Papers*, *50*(3), 397–416. https://doi.org/10.1016/S0967-0637(02)00166-8

Stewart, G., Kirk Cochran, J., Xue, J., Lee, C., Wakeham, S. G., Armstrong, R. A., Masqué, P., & Carlos Miquel, J. (2007). Exploring the connection between 210Po and organic matter in the northwestern Mediterranean. *Deep-Sea Research Part I: Oceanographic Research Papers*, *54*(3), 415–427. https://doi.org/10.1016/j.dsr.2006.12.006

Stewart, G. M., & Fisher, N. S. (2003). Bioaccumulation of polonium-210 in marine copepods. *Limnology and Oceanography*, *48*(5), 2011–2019. https://doi.org/10.4319/lo.2003.48.5.2011

Tang, Y., Castrillejo, M., Roca-Martí, M., Masqué, P., Lemaitre, N., & Stewart, G. (2018a). Distributions of total and size-fractionated particulate 210Po and 210Pb activities along the North Atlantic GEOTRACES GA01 transect: GEOVIDE cruise. *Biogeosciences*, *15*(17), 5437–5453. https://doi.org/10.5194/bg-15-5437-2018

Tang, Y., Castrillejo, M., Roca-Martí, M., Masqué, P., Lemaitre, N., & Stewart, G. (2018b). Distributions of total and size-fractionated particulate 210Po and 210Pb activities along the North Atlantic GEOTRACES GA01 transect: GEOVIDE cruise. *Biogeosciences*, *15*(17), 5437–5453. https://doi.org/10.5194/bg-15-5437-2018

Tang, Y., & Stewart, G. (2019). The 210Po/210Pb method to calculate particle export: Lessons learned from the results of three GEOTRACES transects. *Marine Chemistry*, *217*. https://doi.org/10.1016/j.marchem.2019.103692

Thakur, P., & Ward, A. L. (2020a). 210Po in the environment: insight into the naturally occurring polonium isotope. In *Journal of Radioanalytical and Nuclear Chemistry* (Vol. 323, Number 1, pp. 27–49). Springer Netherlands. https://doi.org/10.1007/s10967-019-06939-2

Thakur, P., & Ward, A. L. (2020b). 210Po in the environment: insight into the naturally occurring polonium isotope. In *Journal of Radioanalytical and Nuclear Chemistry* (Vol. 323, Number 1, pp. 27–49). Springer Netherlands. https://doi.org/10.1007/s10967-019-06939-2

Vajda, N., Larosaa, J., Zeisler, R., Danesi', P., & Kis-Benedek', G. (1997). *A Novel Technique for the Simultaneous Determination of 210Pb and 210Po Using a Crown Ether* (Vol. 37, Number 3).

Vesterbacka, P., & Ikäheimonen, T. K. (2005). Optimization of 210Pb determination via spontaneous deposition of 210Po on a silver disk. *Analytica Chimica Acta*, *545*(2), 252–261. https://doi.org/10.1016/j.aca.2005.04.074

Villa-Alfageme, M., Briggs, N., Ceballos-Romero, E., de Soto, F., Manno, C., & Giering, S. L. C. (2024). Seasonal variations of sinking velocities in Austral diatom blooms: Lessons learned from COMICS. *Deep-Sea Research Part II: Topical Studies in Oceanography*, *213*. https://doi.org/10.1016/j.dsr2.2023.105353

Villa-Alfageme, M., De Soto, F., Le Moigne, F. A. C., Giering, S. L. C., Sanders, R., & García-Tenorio, R. (2014). Observations and modeling of slow-sinking particles in the twilight zone. *Global Biogeochemical Cycles*, *28*(11), 1327–1342. https://doi.org/10.1002/2014GB004981

Villa-Alfageme, M., Mas, J. L., Hurtado-Bermudez, S., & Masqué, P. (2016a). Rapid determination of 210Pb and 210Po in water and application to marine samples. *Talanta*, *160*, 28–35. https://doi.org/10.1016/j.talanta.2016.06.051

Villa-Alfageme, M., Mas, J. L., Hurtado-Bermudez, S., & Masqué, P. (2016b). Rapid determination of 210Pb and 210Po in water and application to marine samples. *Talanta*, *160*, 28–35. https://doi.org/10.1016/j.talanta.2016.06.051

Waples, J. T. (2020). Measuring bismuth-210, its parent, and daughter in aquatic systems. *Limnology and Oceanography: Methods*, *18*(4), 148–162. https://doi.org/10.1002/lom3.10352

Waples, J. T., Hunter, G. J., & Smith, R. A. (2025). Measuring 210Po in natural waters: A comparison of three methods with similar results. *Journal of Environmental Radioactivity*, *288*. https://doi.org/10.1016/j.jenvrad.2025.107732

Wei, C. L., Yi, M. C., Lin, S. Y., Wen, L. S., & Lee, W. H. (2014). Seasonal distributions and fluxes of 210Pb and 210Po in the northern South China Sea. *Biogeosciences*, *11*(23), 6813–6826. https://doi.org/10.5194/bg-11-6813-2014

Xu, R., Li, Q., Liao, L., Wu, Z., Yin, Z., Yang, Y., & Jiang, T. (2022). Simultaneous and efficient removal of multiple heavy metal(loid)s from aqueous solutions using Fe/Mn (hydr)oxide and phosphate mineral composites synthesized by regulating the proportion of Fe(II), Fe(III), Mn(II) and PO43–. *Journal of Hazardous Materials*, *438*. https://doi.org/10.1016/j.jhazmat.2022.129481

Yang, Z., Ma, J., Liu, F., Zhang, H., Ma, X., & He, D. (2022). Mechanistic insight into pH-dependent adsorption and coprecipitation of chelated heavy metals by in-situ formed iron (oxy)hydroxides. *Journal of Colloid and Interface Science*, *608*, 864–872. https://doi.org/10.1016/j.jcis.2021.10.039

Zhong, Q., Puigcorbé, V., Sanders, C., & Du, J. (2020). Analysis of 210Po, 210Bi, and 210Pb in atmospheric and oceanic samples by simultaneously auto-plating 210Po and 210Bi onto a nickel disc. *Journal of Environmental Radioactivity*, *220–221*. https://doi.org/10.1016/j.jenvrad.2020.106301

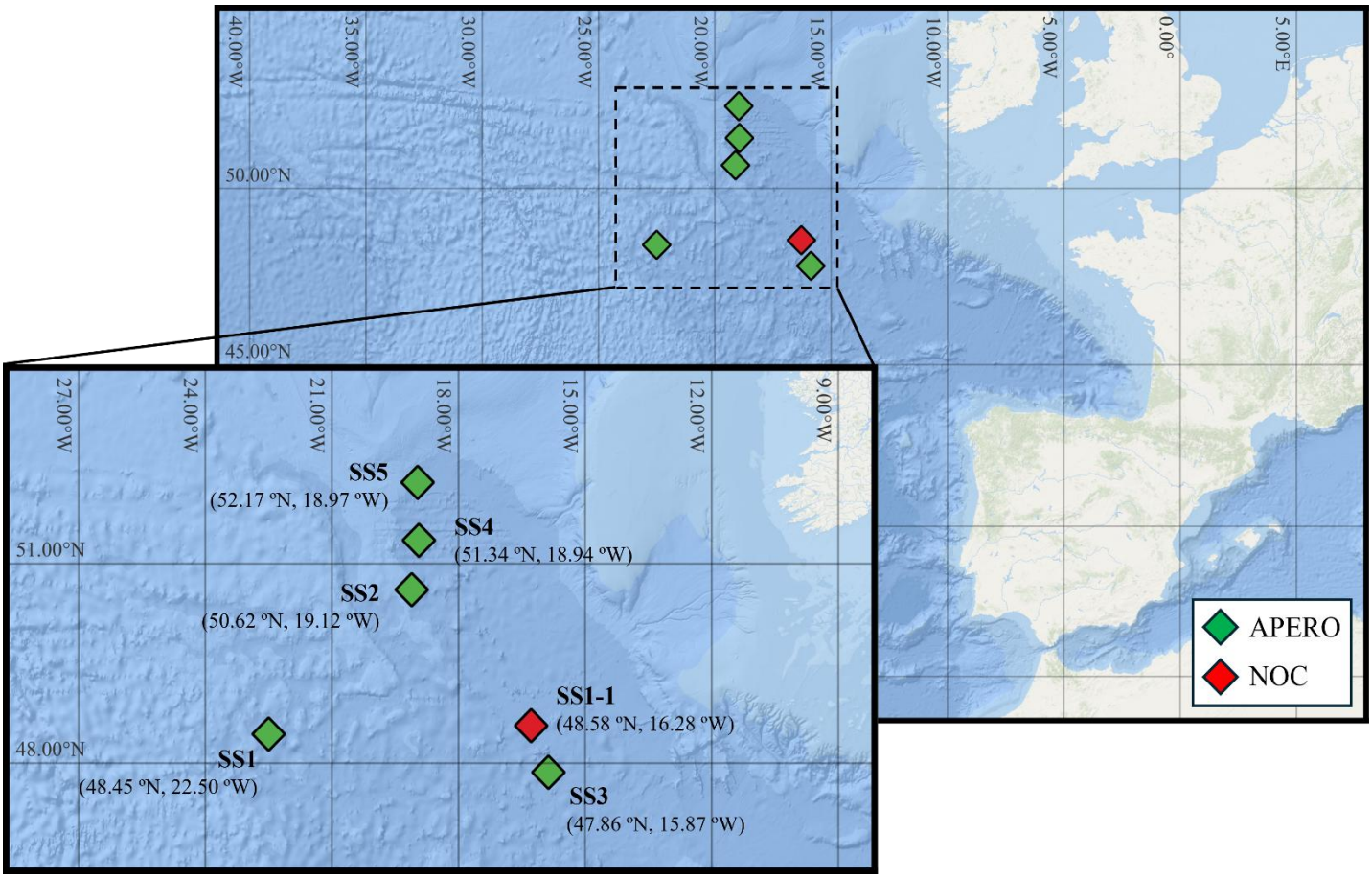

Figure 1. Stations sampled during the NOC (Red) and APERO (Green) campaigns around the PAP-SO in spring 2022 and summer 2023, respectively

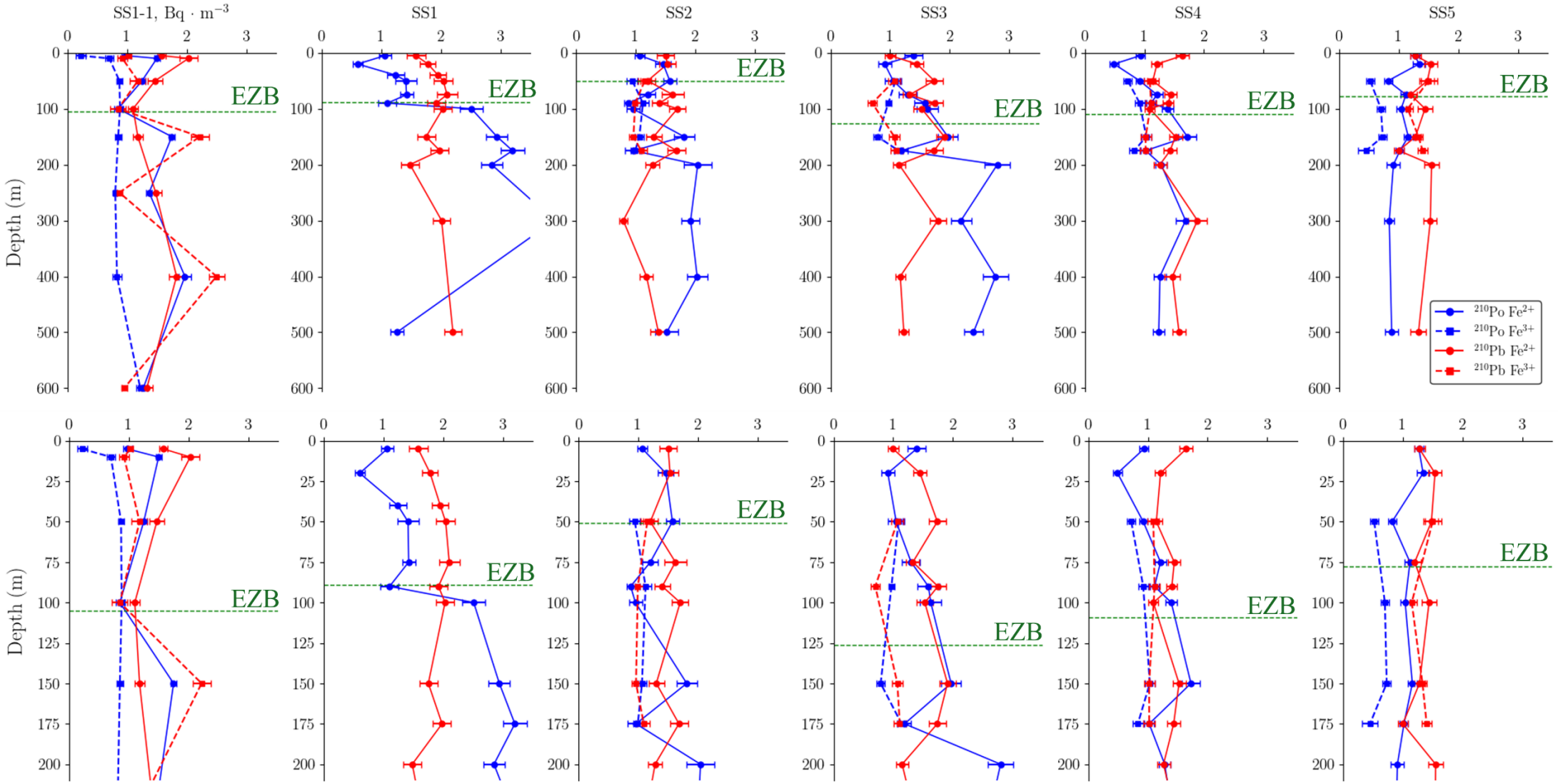

Figure 2. (Top) ^{210}Po (Blue filled circle) and ^{210}Pb (Red filled diamond) activity concentration (Bq · m^{-3}) depth profiles measured with Fe^{2+} (straight line) and Fe^{3+} (dashed line) methods. (Bottom) 200 m - zoom

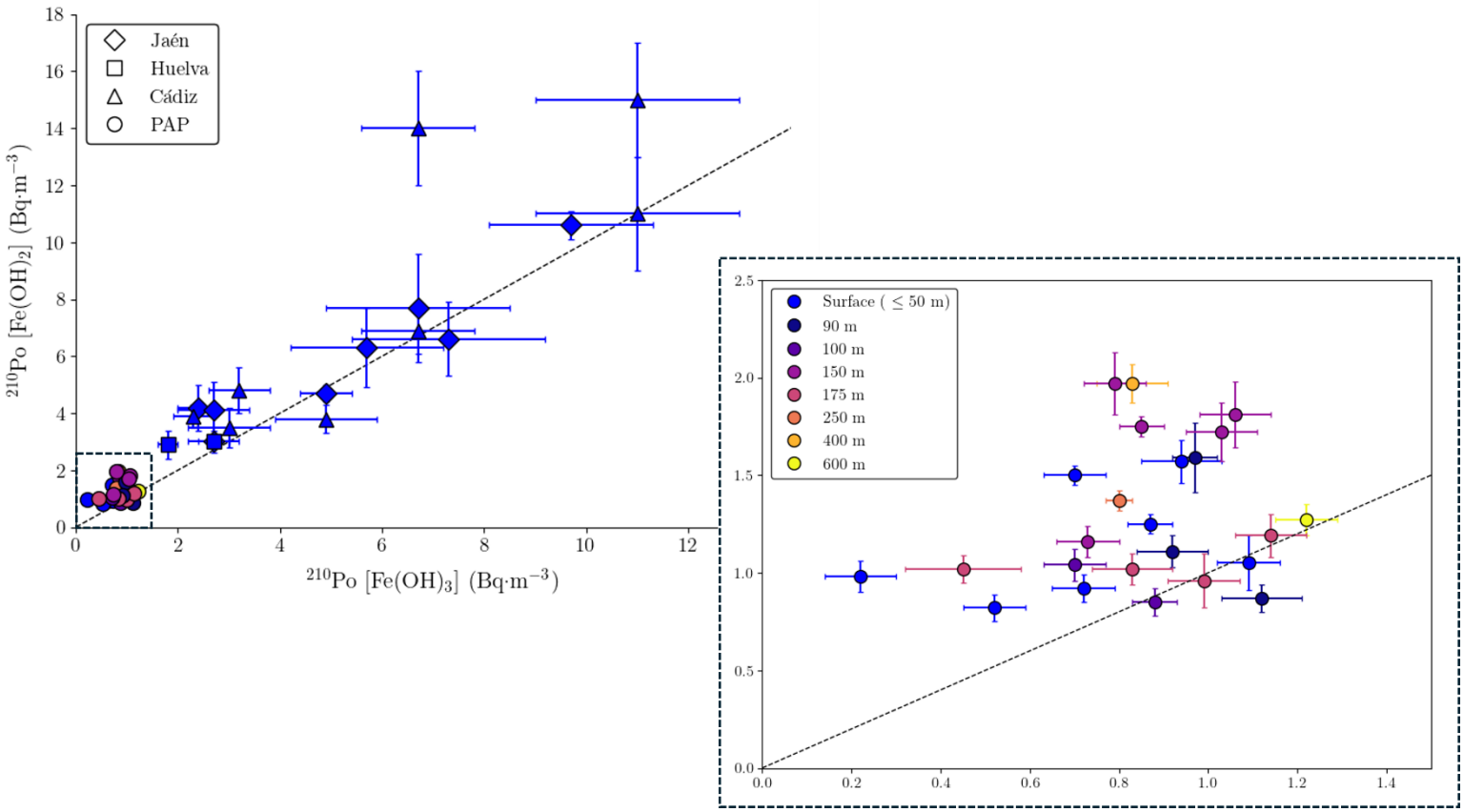

Figure 3. ^{210}Po activity concentrations (Bq · m^{-3}) determined using the Fe^{3+} (x-axis) and Fe^{2+} (y-axis) methods. The 1:1 line ($y = x$, black dashed line) is also plotted. The zoomed figure (lower right) shows the results for open-ocean samples differentiated by depth

Table 1. Total ^{210}Po activity concentrations (Bq·m^{-3}) and chemical yields ($R_{\%}$) obtained with the Fe^{3+} and Fe^{2+} methods in duplicate samples and batch averages from groundwater (Jaén) and surface seawater (Cádiz and Huelva). Uncertainties are reported as absolute values (±σ) and percentages (%)

Study Area	**Batch**	Samples duplicates								Batches average							
		$Fe(OH)_3$				**$Fe(OH)_2$**				**$Fe(OH)_3$**				**$Fe(OH)_2$**			
		^{210}Po	**± σ**	**%**	**$R_{\%}$**	**^{210}Po**	**± σ**	**%**	**$R_{\%}$**	**^{210}Po**	**± σ**	**%**	**$R_{\%}$**	**^{210}Po**	**± σ**	**%**	**$R_{\%}$**
Uranium mine **Jaén, Spain** 38.21 ºN, 4.1 ºW 17/01/2021	A	6.7	1.8	27	36	7.7	1.9	25	60	7.4	1.7	23	48 ± 8	7.8	2.0	26	61 ± 8
		5.7	1.5	26	53	6.3	1.4	26	50								
		7.3	1.9	26	48	6.6	1.3	23	65								
		9.7	1.6	16	55	10.6	0.5	5	68								
	B	2.4	0.4	29	60	4.2	0.8	19	51	2.6	0.1	21	64 ± 4	3.8	0.6	18	53 ± 3
		2.7	0.7	26	66	4.1	1.0	24	56								
		2.7	0.3	11	67	3.0	0.2	7	51								
	C	4.9	0.5	10	45	4.7	0.3	6	55	4.9	0.5	10	45 ± 0	4.7	0.3	6	55 ± 0
		22	4	18	49	18	2	11	54								
Punta Umbría **Huelva, Spain** 37.2 ºN, 7.0 ºW 8/12/2021	D	2.7	0.5	19	55	3.0	0.4	13	55	2.3	0.6	26	64 ± 13	3.0	0.1	3	50
		1.8	0.2	11	73	2.9	0.5	17	44								
Playa de la Cortadura **Cádiz, Spain** 36.5 ºN, 6.3 ºW 18/03/2022	E	3.0	0.8	30	49	3.5	0.7	20	43	2.7	0.5	19	49 ± 0	3.7	0.3	8	50 ± 9
		2.3	0.4	17	49	3.9	0.4	10	56								
	F	6.7	1.1	16	55	6.9	0.8	12	55	4.9	1.8	37	55 ± 3	5.2	1.6	31	52 ± 8
		4.9	1.0	20	50	3.8	0.5	13	59								
		3.2	0.6	19	55	4.8	0.8	17	43								
	G	6.7	1.1	16	55	14	2	14	53	10.7	2.5	23	60 ± 4	13	2	15	50 ± 3
		11	2	18	58	15	2	13	50								
		11	2	18	65	11	2	18	48								

Supplementary Material

Figure S1. (Left) Sampling locations of coastal surface seawater from Cádiz and Huelva. (Right) Groundwater sampling locations in Jaén

Table S1. Total ^{210}Pb, ^{210}Po activities concentration ($Bq \cdot m^{-3}$), $^{210}Po/^{210}Pb$ activity ratios and stations average chemical yield using Fe^{3+} and Fe^{2+} methods in the duplicate samples collected around the PAP-Site during the NOC (SS1-1) and APERO (SS1 to SS5) campaigns. The thick dashed line differentiates EZ values (above) from TZ (below). Chemical yields below 20% were not considered in average values.

Study Area	Depth (m)	^{210}Po ($Bq \cdot m^{-3}$)		^{210}Pb ($Bq \cdot m^{-3}$)		^{210}Po / ^{210}Pb		Average $R_{\%}$	
		$Fe(OH)_3$	**$Fe(OH)_2$**	**$Fe(OH)_3$**	**$Fe(OH)_2$**	**$Fe(OH)_3$**	**$Fe(OH)_2$**	**$Fe(OH)_3$**	**$Fe(OH)_2$**
SS1-1 **PAP-Site** 48.6 ºN, 16.3º W 14/05/2022	5	0.22 ± 0.08	0.98 ± 0.08	1.02 ± 0.05	1.58 ± 0.07	0.22 ± 0.08	0.62 ± 0.06	57 ± 6	35 ± 7
	10	0.70 ± 0.07	1.50 ± 0.05	0.92 ± 0.08	2.03 ± 0.15	0.76 ± 0.10	0.74 ± 0.06		
	50	0.87 ± 0.05	1.25 ± 0.05	1.18 ± 0.13	1.47 ± 0.12	0.73 ± 0.09	0.86 ± 0.08		
	100	0.88 ± 0.05	0.85 ± 0.07	0.85 ± 0.13	1.10 ± 0.08	1.04 ± 0.17	0.77 ± 0.08		
	150	0.85 ± 0.05	1.75 ± 0.05	2.22 ± 0.15	1.18 ± 0.08	0.38 ± 0.03	1.48 ± 0.11		
	250	0.80 ± 0.03	1.37 ± 0.05	0.87 ± 0.05	1.48 ± 0.10	0.92 ± 0.07	0.92 ± 0.07		
	400	0.83 ± 0.08	1.97 ± 0.10	2.50 ± 0.13	1.83 ± 0.13	0.33 ± 0.04	1.07 ± 0.09		
	600	1.22 ± 0.07	1.27 ± 0.08	0.95 ± 0.05	1.33 ± 0.10	1.28 ± 0.10	0.95 ± 0.10		
SS1 **PAP-Site** 48.3 ºN, 22.3 ºW 10/06/2023	5	-	1.06 ± 0.10	-	1.58 ± 0.16	-	0.67 ± 0.09	-	34 ± 9
	20	-	0.60 ± 0.08	-	1.78 ± 0.13	-	0.34 ± 0.05		
	40	-	1.24 ± 0.15	-	1.95 ± 0.14	-	0.64 ± 0.09		
	50	-	1.41 ± 0.18	-	2.04 ± 0.16	-	0.69 ± 0.10		
	75	-	1.42 ± 0.11	-	2.10 ± 0.17	-	0.68 ± 0.08		
	90	-	1.10 ± 0.15	-	1.92 ± 0.15	-	0.57 ± 0.09		
	100	-	2.51 ± 0.19	-	2.03 ± 0.15	-	1.24 ± 0.14		
	150	-	2.94 ± 0.18	-	1.75 ± 0.15	-	1.68 ± 0.17		
	175	-	3.20 ± 0.20	-	1.98 ± 0.15	-	1.62 ± 0.16		
	200	-	2.85 ± 0.18	-	1.48 ± 0.15	-	1.93 ± 0.23		
	300	-	3.9 ± 0.3	-	2.01 ± 0.14	-	1.91 ± 0.20		
	500	-	1.26 ± 0.11	-	2.20 ± 0.14	-	0.57 ± 0.06		
SS2 **PAP-Site** 50.4 ºN 19.1 ºW 16/06/2023	5	-	1.07 ± 0.08	-	1.50 ± 0.14	-	0.70 ± 0.08	40 ± 9	31 ± 7
	20	-	1.46 ± 0.13	-	1.53 ± 0.14	-	0.96 ± 0.12		
	50	0.94 ± 0.09	1.57 ± 0.11	1.15 ± 0.11	1.20 ± 0.12	0.82 ± 0.13	1.31 ± 0.16		
	75	-	1.20 ± 0.13	-	1.62 ± 0.19	-	0.74 ± 0.12		
	90	1.12 ± 0.09	0.87 ± 0.07	0.99 ± 0.09	1.40 ± 0.13	1.13 ± 0.13	0.62 ± 0.08		
	100	-	0.95 ± 0.11	-	1.70 ± 0.14	-	0.56 ± 0.08		
	150	1.06 ± 0.08	1.81 ± 0.17	0.96 ± 0.07	1.30 ± 0.13	1.10 ± 0.11	1.40 ± 0.20		
	175	0.99 ± 0.08	0.96 ± 0.14	1.09 ± 0.10	1.68 ± 0.15	0.91 ± 0.12	0.57 ± 0.10		
	200	-	2.04 ± 0.24	-	1.28 ± 0.12	-	1.59 ± 0.24		
	300	-	1.92 ± 0.15	-	0.79 ± 0.07	-	2.4 ± 0.3		
	400	-	2.03 ± 0.17	-	1.18 ± 0.11	-	1.71 ± 0.22		
	500	-	1.52 ± 0.19	-	1.38 ± 0.13	-	1.10 ± 0.17		

SS3 **PAP-Site** 47.8 ºN 15.5 ºW 22/06/2023	5	-	1.39 ± 0.15	-	1.00 ± 0.09	-	1.38 ± 0.20	57 ± 10	40 ± 6
	20	-	0.91 ± 0.11	-	1.45 ± 0.11	-	0.63 ± 0.09		
	50	1.09 ± 0.07	1.05 ± 0.14	1.07 ± 0.10	1.74 ± 0.14	1.01 ± 0.12	0.60 ± 0.10		
	75	-	1.30 ± 0.15	-	1.33 ± 0.11	-	0.98 ± 0.14		
	90	0.97 ± 0.05	1.59 ± 0.18	0.70 ± 0.08	1.75 ± 0.13	1.39 ± 0.17	0.91 ± 0.12		
	100	-	1.63 ± 0.18	-	1.53 ± 0.14	-	1.07 ± 0.15		
	150	0.79 ± 0.07	1.97 ± 0.16	1.07 ± 0.09	1.91 ± 0.14	0.74 ± 0.11	1.03 ± 0.11		
	175	1.14 ± 0.08	1.19 ± 0.11	1.11 ± 0.10	1.74 ± 0.14	1.03 ± 0.12	0.69 ± 0.08		
	200	-	2.80 ± 0.21	-	1.15 ± 0.10	-	2.4 ± 0.3		
	300	-	2.19 ± 0.17	-	1.80 ± 0.14	-	1.22 ± 0.13		
	400	-	2.77 ± 0.21	-	1.17 ± 0.08	-	2.37 ± 0.25		
	500	-	2.40 ± 0.16	-	1.23 ± 0.08	-	1.95 ± 0.19		
SS4 **PAP-Site** 51.1 ºN 18.5 ºW 3/7/2023	5	-	0.93 ± 0.08	-	1.64 ± 0.11	-	0.56 ± 0.06	41 ± 4	42 ± 13
	20	-	0.49 ± 0.08	-	1.21 ± 0.09	-	0.40 ± 0.07		
	50	0.72 ± 0.07	0.92 ± 0.07	1.09 ± 0.10	1.14 ± 0.10	0.66 ± 0.12	0.81 ± 0.09		
	75	-	1.21 ± 0.10	-	1.44 ± 0.10	-	0.84 ± 0.09		
	90	0.92 ± 0.08	1.11 ± 0.08	1.11 ± 0.09	1.40 ± 0.09	0.83 ± 0.11	0.79 ± 0.08		
	100	-	1.39 ± 0.10	-	1.09 ± 0.08	-	1.27 ± 0.13		
	150	1.03 ± 0.08	1.72 ± 0.15	1.02 ± 0.09	1.52 ± 0.11	1.01 ± 0.12	1.13 ± 0.13		
	175	0.83 ± 0.09	1.02 ± 0.08	1.02 ± 0.10	1.43 ± 0.11	0.81 ± 0.13	0.72 ± 0.08		
	200	-	1.28 ± 0.09	-	1.26 ± 0.11	-	1.01 ± 0.11		
	300	-	1.69 ± 0.16	-	1.89 ± 0.16	-	0.90 ± 0.11		
	400	-	1.26 ± 0.10	-	1.47 ± 0.13	-	0.86 ± 0.10		
	500	-	1.24 ± 0.10	-	1.58 ± 0.11	-	0.78 ± 0.08		
SS5 **PAP-Site** 51.5 ºN 19.2 ºW 10/7/2023	5	-	1.27 ± 0.08	-	1.28 ± 0.09	-	0.99 ± 0.10	49 ± 6	40 ± 7
	20	-	1.34 ± 0.10	-	1.54 ± 0.11	-	0.87 ± 0.09		
	50	0.52 ± 0.07	0.82 ± 0.07	1.50 ± 0.15	1.48 ± 0.11	0.35 ± 0.12	0.55 ± 0.06		
	75	-	1.12 ± 0.09	-	1.20 ± 0.11	-	0.94 ± 0.11		
	100	0.70 ± 0.07	1.04 ± 0.08	1.15 ± 0.09	1.44 ± 0.12	0.61 ± 0.10	0.72 ± 0.08		
	150	0.73 ± 0.07	1.16 ± 0.08	1.33 ± 0.07	1.28 ± 0.09	0.55 ± 0.09	0.91 ± 0.09		
	175	0.45 ± 0.13	1.02 ± 0.07	1.40 ± 0.08	1.00 ± 0.08	0.32 ± 0.14	1.02 ± 0.10		
	200	-	0.91 ± 0.11	-	1.55 ± 0.12	-	0.58 ± 0.09		
	300	-	0.84 ± 0.08	-	1.53 ± 0.11	-	0.55 ± 0.06		
	500	-	0.88 ± 0.11	-	1.33 ± 0.13	-	0.66 ± 0.11		

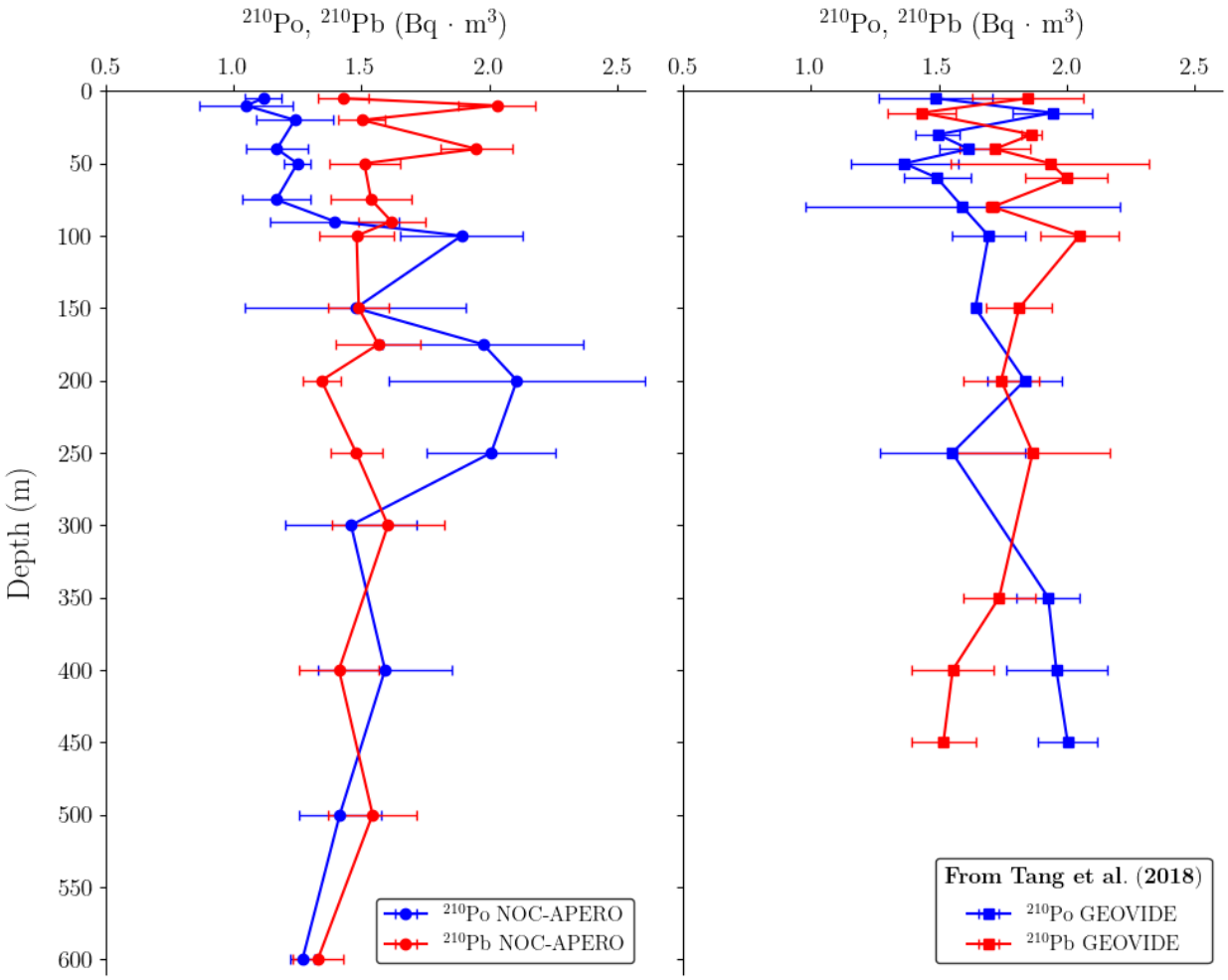

Figure S2. (Left) Average ^{210}Po and ^{210}Pb activity concentrations (Bq·m^{-3}) determined during the NOC and APERO campaigns. (Right) Average ^{210}Po and ^{210}Pb activity concentrations determined at Stations 21 and 26 along the GEOVIDE cruise in the North Atlantic reported in (Tang et al., 2018).

Equations from Section 2.3.4.

For simplicity of notation, subscripts 1, 2, 3, and 4 refer to ^{210}Pb, ^{210}Bi, ^{210}Po and ^{209}Po, respectively, in the following equations,

$$A_{31}(t_1) = \frac{C_b}{C_a} \cdot A_1(t_2) \tag{S1}$$

$$A_1(t_s) = \frac{C_a}{C_c} \cdot A_3(t_2) \cdot exp[\lambda_1 \cdot (t_2 - t_s)] \tag{S2}$$

Where,

$$C_a = \frac{(\lambda_3 - \lambda_2)(\lambda_3 - \lambda_1)(\lambda_2 - \lambda_1)}{\lambda_2 \lambda_3},$$

$$C_b = [(\lambda_3 - \lambda_2) \cdot exp[-\lambda_1(t_2 - t_1)] - (\lambda_3 - \lambda_1)] \cdot exp[-\lambda_2(t_2 - t_1)] + (\lambda_2 - \lambda_1) \cdot exp[-\lambda_3(t_2 - t_1)]]$$

$$C_c = [(\lambda_3 - \lambda_2) \cdot exp[-\lambda_1(t_2 - t_s)] - (\lambda_3 - \lambda_1)] \cdot exp[-\lambda_2(t_2 - t_s)] + (\lambda_2 - \lambda_1) \cdot exp[-\lambda_3(t_2 - t_s)]]$$